Modeling and Identification of Air Suspension in Heavy-Duty Vehicles

Carl-Philip Lartén

LINKÖPING UNIVERSITY

Master of Science Thesis in Electrical Engineering

Modeling and Identification of Air Suspension in Heavy-Duty Vehicles

Carl-Philip Lartén

LiTH-ISY-EX--16/4996--SE

Supervisor: **Gustav Lindberg**
ISY, Linköpings universitet

Stefan Sappei
Scania CV AB

Examiner: **Johan Löfberg**
ISY, Linköpings universitet

Division of Automatic Control
Department of Electrical Engineering
Linköping University
SE-581 83 Linköping, Sweden

Abstract

A heavy-duty vehicle can benefit from the height control of the chassis that an air suspension provides. For example, to retain a pitch angle parallel to the road, regardless of what load it carries. For the purpose of developing a controller, a model of the air suspension provides evaluation and testing opportunities as well as it gives the option for more advanced model based controller algorithms. Furthermore, a model can provide with an accurate axle weight estimation. In this thesis, both physical and statistical models are developed and parameters are estimated by solving minimization problems. They are then evaluated using data collected from a Scania truck, comparing normalized mean-root error values as well as residual analysis of each model.

Acknowledgments

Contents

Notation

PHYSICAL CONSTANTS

Notation	Meaning
g	Standard gravity
R	Universal gas constant

PARAMETERS

Notation	Meaning
T	Temperature inside the bellow
V	Geometrical volume of the bellow
p_{amb}	Ambient pressure
h_0	Height between the chassis and the hinge
l_1	Length between the axle and the hinge
l_2	Length between the axle and the bottom of the bellow
l_3	Length between the axle and the damper
A	Average cross-sectional area of bellow
h_{bellow}	Height between the centre of the bottom and top of bellow
h_{axle}	Height between the axle and the chassis
m_{tot}	The total mass carried by one suspension
m_1	The part of the total mass that is sprung
m_2	The part of the total mass that is unsprung
k_l	The gain corresponding to the levers effect on the system
k_f	Friction constant
I_g	The rotational inertia of the lever
$\boldsymbol{r_{aG}}$	The distance vector between the hinge and the gravitational center of the mass
k_{scl}	Spring constant of lever
k_w	Spring constant of wheel
A_{eff}	Effective area of bellow

Variables

Notation	Meaning
x_1	The vertical distance between the ground and the top of the bellow in QCM 1
x_2	The vertical distance between the ground and the bottom of the bellow in QCM 1
x	The vertical distance between the ground and the hinge in QCM 2
α	Angle position of lever in QCM 2
a_g	The acceleration of m_2 in QCM 2
F_{ab}	Force from the bellow
F_d	Force from the damper
F_w	Force from the wheel
p_{in}	Pressure inside the bellow
n	Number of air particles in bellow
f_{air}	Air flow into and out of the bellow

Abbreviations

Abbreviation	Meaning
HDV	Heavy-Duty Vehicle
QCM	Quarter Car Model
ARX	Auto-Regression eXtended
ARMAX	Auto Regression Moving Average eXtended
BJ	Box-Jenkins
OE	Output-Error
NRMSE	Normalized Root-Mean-Square-Error

1
Introduction

This master's thesis concerns modeling of an air suspension, with future development of a controller algorithm in mind. The thesis was done at Scania CV AB, as a part of a master's degree at Linköpings Universitet.

1.1 Background

Scania means "Skåne" (province in the south of Sweden) in Latin and is where the company started in 1900, building bikes and short there after cars and trucks. Earlier in 1891 a company called Vabis was founded in Södertälje, Sweden, set out to manufacture goods wagons for railway usage. Later in 1911 the two companies fused and produces today, 105 years later, trucks, buses and industrial engines at several locations around the world, selling the products globally. The company stands on their three core values, customer first, respect for the individual and quality. [2] Scania was market leader in Sweden with more than 45 % of the sales in October 2015 [15] and is one of the market leaders in Europe.

Heavy-Duty Vehicles (HDV) are a key ingredient to maintain functioning infrastructure and therefore society, delivering whatever we buy from wherever the product is produced. They make sure that the consumer has their fresh food in the store or becomes the package they ordered over the Internet, maybe from the other side of the world.

HDVs use air suspension to benefit from the advantage of a steady ride height, pitch of the truck and control of loading height. When loading a truck with several tons on one axle, a height difference between the axles will take place if the suspension is not controlled. To maintain the height, the air suspension can automatically be inflated or deflated. This can also be beneficial when used manually by the driver, for example when adjusting the height of the truck to different loading docks. Frequently used height-settings can be stored, which

will speed up the loading process. Another scenario when height adjustment by controlling the air auspension is when a truck dumps it's load while driving, for example salt to prevent icy-roads.

With the use of different sensors the axle weight can be estimated. This weight estimation is frequently used by drivers that wants to maximize the use of the load capacity as well as not exceed possible road restrictions. A model of the system can be used to estimate this weight.

To develop a controller managing the stated usage of an air suspension, it is highly beneficial to have a model of the air suspension. Both for the purpose of testing and tuning controller algorithms, but also because a model gives the opportunity to evaluate more complex model based controllers.

1.2   Problem Formulation

The goal of this master's thesis is to enable the design of a controller algorithm that uses the advantages given by an air suspension to retain or adjust the trucks height. The model developed should be accurate enough for the developer to evaluate different controller methods. The model is developed in `MATLAB`/`Simulink` and estimated and validated using data collected through tests done with a truck from Scania CV AB.

When a truck is loaded it can be seen in Figure 1.2 that the height of the truck decreases accordingly. This can be avoided by controlling the air flow into the air bellows. The data in the figure is collected when the test truck in Figure 1.1 is loaded with one ton at a time with the help of a traverse.

Figure 1.1: The truck used for data colleciton, of type Scania R620.
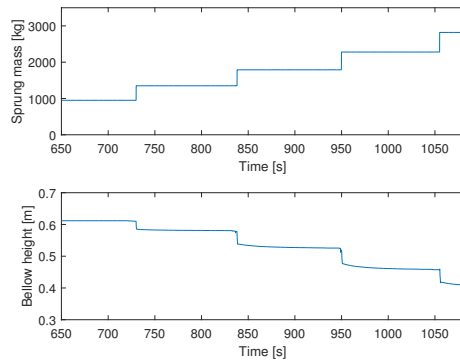
Figure 1.2: When the truck is loaded, the height of the bellow decreases.

In order to help the development of a controller algorithm and a weight estimation, the model should meet the following requirements:

- The model should estimate the change in pressure and height when unloading/loading weight on/off a truck.

- The model should be able to estimate the change in pressure and height when the solenoid valve controlling the air flow lets air in or out of the air bellow.

- The model should be able to estimate the change in pressure and height from road input (secondary).

Another goal with the thesis is to obtain an understanding of the system for the future work of creating a level controller.

How well the model needs to simulate the true system depends on the end usage of it. For the purpose of testing and tuning a controller a highly accurate model is most likely not necessary, but in the case of model based controller algorithms or weight estimation a highly accurate model would increase the controller's or estimator's performance significantly.

1.3   Method

To create a model that should be able to estimate a specific system's behaviour, it is necessary to have relevant data collected. This is also important for validation purposes. A part of the work with the thesis is collection of data with a Scania R620 truck.

modeling the air suspension, mainly physical modeling is done, which describes the systems behaviour through physical relationships. In addition, statistical modeling is done in combination with physical modeling, where pre-defined mathematical equations are fitted to estimation data.

A general method for modeling of a system is proposed in [7], which was followed throughout the thesis. The process is presented in Figure 1.3.

In Figure 1.3 the structuring of the system refers to defining the different parts that need to be modeled, as well as the parameters that need to be set. Some of the system's parts influence on the output might be small compared to other parts or the dynamic of it might not be of interest, and can thus be neglected or simplified. If a statistical model is used its parameters must be estimated. This can also be the case for some physical parameters, which might in reality be hard to measure directly. To know how well the model represents the true system it needs to be validated against collected data. As seen in the flowchart, modeling a system is usually done iteratively. It is common to go back and fourth between the steps and try new approaches to iteratively improve the model based on findings in the validation part, which also is the case in this thesis.

1.4   Delimitations

The following delimitations are established, when considering the time span and complexity of the tasks.
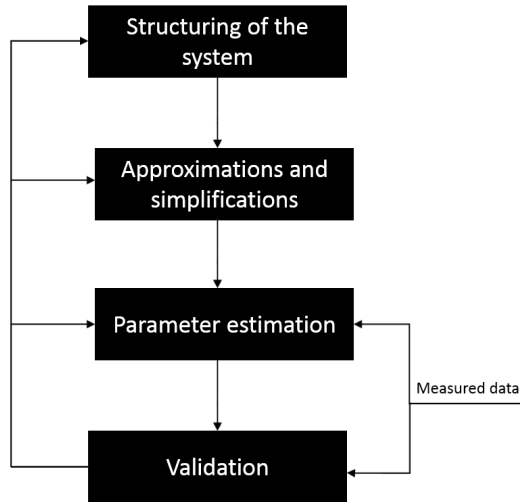
Figure 1.3: *Proposed method for modeling, presented as a flow chart.*

- The model should only simulate the movement of one isolated suspension setup with one air bellow. This means that any eventual disturbance from the rest of the chassis is not considered.

- Leveling considers only the height difference between axles, not the height difference from side to side of the truck.

- Disturbances in the measured signal shall not be modeled.

2

System Description

An HDV comes in many different configurations for different purposes. Some of the important setup choices that a buyer must make are the number of axles, how many wheels should deliver traction force and how many axles should be leaf contra air suspended. The many configuration possibilities of Scania trucks must be taken into consideration when a model is develop. The air suspension modeled in this thesis and used on the truck in Figure 1.1, and physical parameters used by the model are defined in this chapter.
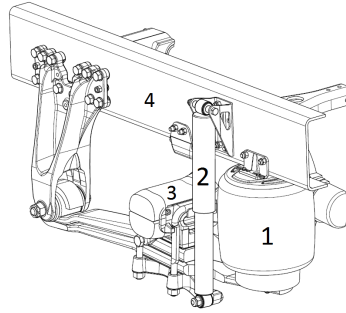
2.1   Air Suspension

In Figure 2.1 the air suspension which is modeled is presented. The figure shows the suspension setup viewed from the long side of the truck, where the front end of the truck would be located to the left.

The lever that the axle sits on is a leaf spring. This means that the shape of the lever changes with applied load, changing the geometrical relations of the system.

One axle's two bellows are connected to the same air-circuit and there is only one height and pressure sensor per axle. To obtain observability of the height of the whole axis, the pressure must be assumed to be constant over the whole air-circuit.

Some air springs are inflatable/deflatable for the purpose of changing the characteristics of the spring, which correspond to changing the stiffness of the bellow [14][9]. The purpose of the air spring that is modeled in this thesis is to control the height. When air is let out of the air bellow (1 in Figure 2.1) to lower the truck, the air bellow folds into itself and the other way around when air is added. Figure 2.2 shows the principal of the inside of a typical bellow, although it is not identical to the bellow used in the thesis.

Figure 2.1: *Scanias air suspension setup. 1) air bellow, 2) damper, 3) axle, 4) chassis.*
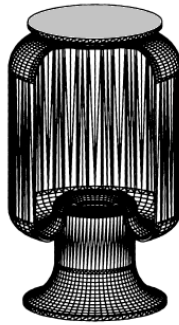
Figure 2.2: *Conceptual illustration of a typical air bellow which can be folded into itself.*

The air bellow is made of an elastic material, in this case a kind of rubber. Some nonlinearities comes from how the bellow is installed, for example the bottom of the suspension moves in a circular manner, rather than straight up and down[12]. This gives the air bellow different shapes depending on the height. The elastic material is connected to a cylinder which can move in and out of the bellow and is connected to the axle through the lever.

2.2   Actuators and Sensors

For the purpose of collecting data and controlling the air suspension, one actuator and three sensors are of interest.

2.2.1   Valve

To let air in and out to and from the bellow, there is a valve between the bellow and a source of compressed air. The valve has one channel for air flow into the bellows and another channel for air flow out of the bellows. Altogether the valve can assume three states: air in, air out and closed. On the test-truck the valve is coupled to both air bellows on the axle.

As the valve has only three discrete states, there are two possibilities for controlling the mass of air flowing into the bellow when opening the valve. The first would be by controlling the pressure in the air-tank-supply. Unfortunately this method can directly be discarded as an option, as this pressure can not be controlled [12]. The second option is to open and close the valve at higher frequencies to control the amount of air flowing through the valve. This alternative puts high demands on the durability of the valve. According to [12] the valve is not meant to and can not endure such strains. Thus restraining the options for controlling the air flow.

2.2.2   Height Sensor

The height sensor shows the height between the axle and the chassis. It does so through a two-link arm that generates an angle given through a potentiometer and every angle corresponds to a pre-defined height. There is one height sensor per axle, located on the left side of the modeled axle. The height sensor has a sample time of 100 [ms] and a resolution of 0.1 [mm].

As the height sensor mounted on the truck is known to be non-exact, with at least an offset error, the test truck is equipped with another sensor as well. This ensures that the height is measured correctly with calibrated equipment. The second height sensor is a potentiometer and gives a linear relation between height and voltage, which is dependent on how far a wire is pulled out. This wire is connected to a spring driven wheel, pulling the wire back in when the height is decreased. The height sensor was connected between the axle and the chassis.

2.2.3   Pressure Sensor

The pressure sensor mounted on the air bellow gives the relative pressure between the bellow and atmosphere. The signal measured has a sample time of 100 [ms] and a resolution of 0.1 [kPa]. There is one pressure sensor installed per axle, on the bellow of the left side of the truck relative to the driving direction.

The compressed air source, or actuator tank, is used by the parking break, service break and the air suspension. The pressure just before the valve is not measured directly, a pressure is measured at the point where the air flow branches out to the different functions from the tank, as seen in Figure 2.3. The dynamic opening in the figure requires a pressure of 850 [kPa] to be opened. According to [13], this pressure sensor gives a good estimate of the supply pressure to the air suspension when the pressure is static, but when the air is consumed by the air suspension it is less accurate.
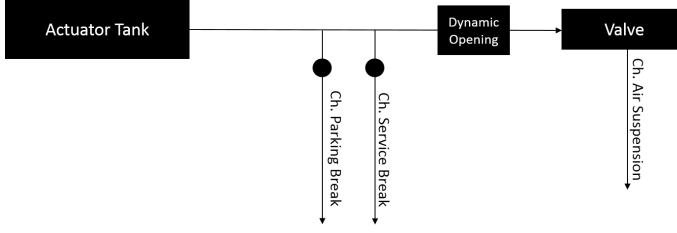
Figure 2.3: Schematic figure over the air circuit, round dots symbols the pressure sensors.

2.3 Geometric Parameters

The geometrical parameters that are used throughout the thesis are presented in Figure 2.4.
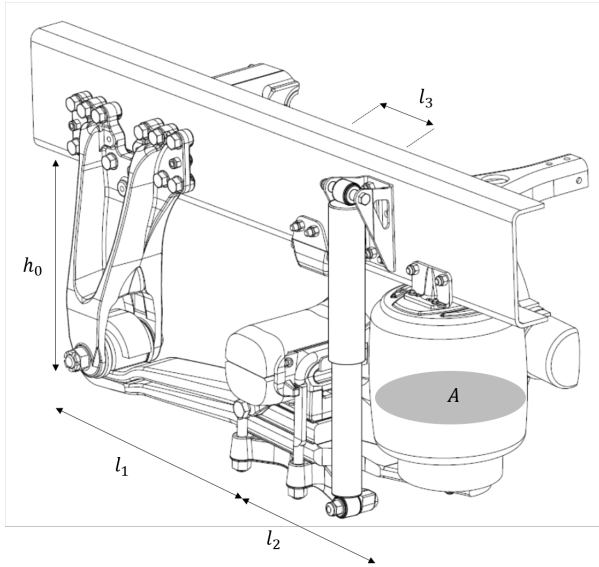
Figure 2.4: Geometrical parameters.

The parameter $h_0[m]$ represents the distance between the bottom of the chassis and the hinge, $l_1[m]$ the distance along the lever between the hinge and the center of the axle, $l_2[m]$ the distance along the lever between the center of the axle to the center of the air bellow and $l_3[m]$ the distance along the chassis between the center of the axle to the center of the damper. Finally, the parameter $A[m^2]$ is the cross-section area of the air bellow.

2.4   Geometric Relations

Two geometric relations are frequently used throughout the thesis to define the height of the bellow. As the measured height is the height between the axle and chassis, the equations that describes the bellow height h_{bellow} in Figure 2.5 are needed.
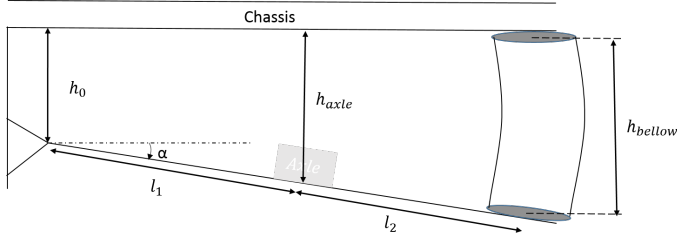
Figure 2.5: *Geometrical relations.*

By proportionality of triangles, the relation between the height h_{axle} and h_{bellow} is given by

$$h_{bellow} = h_0 + \frac{l_1 + l_2}{l_1}(h_{axle} - h_0). \tag{2.1}$$

Note that this only holds when the lever has no load acting on it, this is taken into account statically with the help of knowing the spring characteristics of the lever. The relation between the angle of the lever α and the height of the bellow h_{bellow} is also frequently used and can be defined as

$$h_{bellow} = h_0 + (l_1 + l_2)sin(\alpha). \tag{2.2}$$

3

Modeling

There are several methods for modeling a system. One of them is to use the laws of physics to describe the system and use experimental data or given information about the system to determine the system's parameters. Another way is to use black-box modeling to describe the whole or parts of the system. Black-box modeling is when the relation between input and output is described through a model class and the parameters estimated through statistical methods with the help of experimental data. Thereafter the model is compared against a new data set, to see how well the model describes the true system. This is done without the need of knowing the underlying physical relations. Finally, there is the alternative that is known as grey-box modeling, where the parameters have physical interpretations but are estimated through statistical methods. This can be described as a mix between black-box and physical modeling methods. [7]
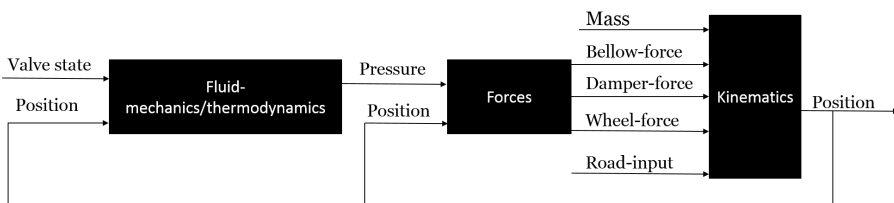
Figure 3.1: *An overview of the relations between inputs and outputs.*

In Figure 3.1 an overview is given of the relations that are to be modeled. The mass corresponds to what load is put on the truck. The valve state control input, as described in 2.2.1, specifies if the valve should let air into the bellow, out of the bellow or should be closed. The input "Road-input" corresponds to changes in the height of the road.

The three blocks in the overview can be seen as building blocks which gives a

good idea of how the whole model is built. Each block can be modeled independently and several model combinations are evaluated.

In this thesis all three mentioned methods are used to model the system and sometimes a combination between two or all methods. In this chapter the theory behind each method is described as well as the theory behind the validation methods.

3.1   Physical Modeling

In Figure 3.1 the system is intuitively divided into three parts and for the purpose of physical modeling divided into three areas of physics, which also describes the structure of this section.

- The kinematics of the system, which describes the movement of the system's components depending on forces acting on the system.

- The forces that mainly comes from the air bellow, damper, gravity and the force from the tire.

- The third part is the thermodynamics and fluid mechanics of the system, describing the air-flow in and out of the bellow as well as the pressure in the bellow.

Under this section the submodels created through physical modeling are described, as well as te static relations that are used.

3.1.1   Kinematics

The Quarter-Car-Model (QCM) is well known and often used (for example in [3][10][5]) for modeling suspensions, but as it is a general air suspension model it might not represent the true system sufficiently well. Therefore an additional model is developed, corresponding better to the true system with the same degrees of freedom and parameters as to the true system and directly translatable to the true system. This model also provides more intuitive parameters, making them easier to specify. The second model uses the same principal, modeling a quarter of a car, and will thus from here on be called QCM 2 and the first model QCM 1.

QCM 1

A QCM, (visualized in Figure 3.2) represents one suspension or half an axle of a car or a truck and divides the mass of that quarter of a car into two, one sprung mass (m_1) and one unsprung mass (m_2). It is not fully clear what can be defined as unsprung and sprung mass of the trucks mass, which is why m_2 will be left as a tuning parameter and m_1 being related to m_2 and the total mass on the wheel m_{tot} as

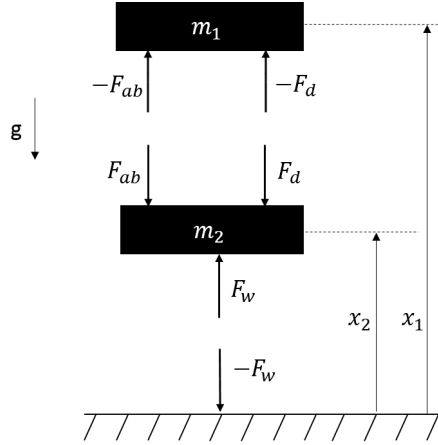$$m_1 = m_{tot} - m_2. \tag{3.1}$$

Newton's First Law of Motion,

$$m\ddot{x} = F, \tag{3.2}$$

applied to the QCM 1 model gives

$$m_1\ddot{x}_1 = -m_1g - F_{ab} - F_d \tag{3.3a}$$

$$m_2\ddot{x}_2 = F_w - F_{ab} - F_d - m_2g, \tag{3.3b}$$

where x_1 and x_2 are the positions of m_1 and m_2 relative to the ground, F_{ab} the force form the air bellow and F_d the damper force.

Figure 3.2: Schematics of QCM 1.

Something crucial that is not considered in this model is the fact that the bellow acts on the axle through a lever. In order to take this into consideration, the force from the bellow is multiplied with a gain that corresponds to the lever. Looking at Figure 2.4, it can be seen that the torque developed by the bellow on the axle through the lever, is equivalent to the bellow's force with the gain $k_l = \frac{l_1+l_2}{l_1}$. Another aspect that is considered is the friction from the hinge that the lever is connected to. This friction is assumed to be proportional to the difference in the vertical speed of the two masses. The proportional parameter k_f is therefore introduced. This results in the updated equations

$$m_1\ddot{x}_1 = -m_1g - k_lF_{ab} - F_d - (\dot{x}_1 - \dot{x}_2)k_f \tag{3.4a}$$

$$m_2\ddot{x}_2 = F_w - k_lF_{ab} - F_d - m_2g. \tag{3.4b}$$

Here, the height of the bellow h_{bellow} is given by

$$h_{bellow} = x_1 - x_2. \tag{3.5}$$

QCM 2

The second method, or model, has state and position variables more translatable to the true system with some neglected attributes. The weight of the lever and the arm holding the lever is neglected and instead included in the weights m_1 and m_2. Mathematically QCM 2 is described via Newton's Law of Motion in (3.2) and Euler's Second Law of Motion in (3.7) and has two degrees of freedom. The first, x, represents the distance between the chassis and the ground and the second, α, the angle of the lever, visualized in Figure 3.3.
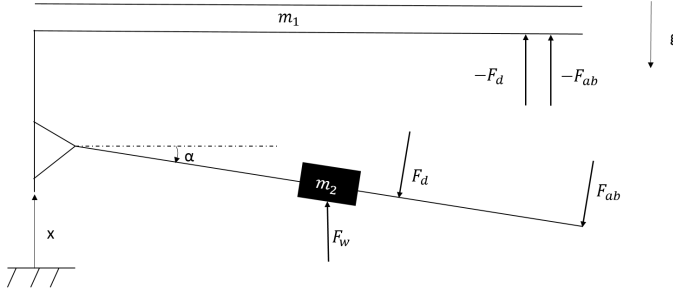

Figure 3.3: A schematic of the QCM 2 model.

In this approach m_2 represents the axles weight, which can be translated to the unsprung mass in QCM 1. The rest of the weight m_1 can be compared to QCM 1's sprung mass, although what is sprung and what is unsprung is not as well defined. The lever's spring characteristics are not dynamically modeled, but instead statically, by equation (3.14).

Equation (3.6) describes the vertical dynamics of the whole system derived from (3.2),

$$(m_1 + m_2)\ddot{x} = F_w - (m_1 + m_2)g. \tag{3.6}$$

In Figure 3.4 the lever is isolated to be able to describe the rotation of the lever in equation (3.11). The forces $F_{A,y}$ and $F_{A,x}$ are the forces from the hinge attached to the chassis acting on the lever.
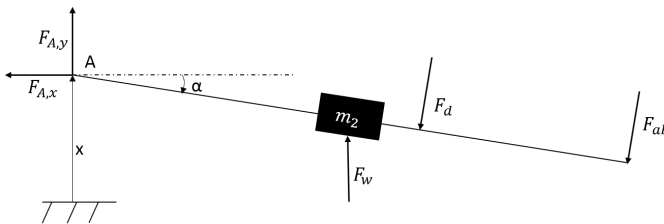
Figure 3.4: A schematic of the lever, isolated from the rest of the system.

To derive the torque with respect to the angular acceleration around the non-fixed point A and the mass's acceleration in Figure 3.4, Euler's Second Law of

Motion is used. For a non-fixed point the torque M_A is defined as

$$M_A = I_g \ddot{\alpha} + m_2 r_{Am_2} \cdot a_{m_2}. \tag{3.7}$$

The rotational inertia I_g is initially estimated as

$$I_g = m_2 r_{Am_2}^2, \tag{3.8}$$

but is left as tuning parameter. The vector r_{Am_2} corresponds to the vector from point A to the center of mass m_2 and a_g to the acceleration at gravitational center of m_2. Then $a_{g\perp}$ is defined as

$$a_{m_2\perp} = a_{m_2} \cdot \hat{\alpha}, \tag{3.9}$$

where $\hat{\alpha}$ is the unit vector of α. There is no relative motion between the system and the ground, thus is a_{m_2} described by

$$\begin{aligned}
a_{m_2} &= a_A + \alpha x r_{Am_2} - \omega^2 r_{Am_2}, \\
a_{m_2\perp} &= -\ddot{x}cos(\alpha) + \alpha l_1 - 2l_1\dot{\alpha}^2 sin(\alpha)cos(\alpha),
\end{aligned} \tag{3.10}$$

where $\omega = \dot{\alpha}$. For the system described in Figure 3.4 the torque, with respect to the forces acting on the system, is given by

$$M_A = l_1 cos(\alpha)(m_2 g - F_w) + (l_1 + l_3)F_d + (l_1 + l_2)F_{ab}. \tag{3.11}$$

Combining and rearranging the two equations (3.7) and (3.11) gives the angular acceleration $\ddot{\alpha}$,

$$\ddot{\alpha} = \frac{l_1 cos(\alpha)(m_2 g - F_w) + (l_1 + l_3)F_d + (l_1 + l_2)F_{ab} - m_2 r_{Am_2}a_{g\perp}}{I_g}. \tag{3.12}$$

Finally, the height of the bellow, defined in (2.2), is given by

$$h_{QCM2} = h_{bellow} = h_0 + sin(\alpha)(l_1 + l_2). \tag{3.13}$$

The parameters h_0, l_1, l_2, l_3 in equations (3.10)-(3.13) refers to the parameters defined in section 2.3.

Leaf Sprung Lever

The lever itself is a leaf spring which is modeled statically. A spring constant k_{scl} of the lever has been estimated at Scania which describes the spring characteristics at the point where the axle is attached to the lever. As mentioned in 2.4 the stated geometrical relations are defined for a stiff lever, but the lever creates an extension in the height h_{axle} depending on the mass put on the wheel. This is simplified as a static extension defined as

$$\Delta h = k_{scl} m_{tot} g. \tag{3.14}$$

3.1.2   Forces

The forces acting on the system which builds up the kinematic equations in 3.1.1 are found both from physical relations and measured data found at Scania.

Wheel Force

The wheel force is commonly modeled as a spring, for example in [3][4][10], and is so in this thesis as well. The force from the wheel acting on the axle (or unsprung mass) is therefore given by

$$F_w = k_w \Delta r, \tag{3.15}$$

where the spring-constant k_w is given by Scania. As any spring the wheel force depends on it's radial compression or extension of the wheel Δr from its unloaded state. As the tire can't pull the truck down, (3.15) is only defined for $\Delta r \geq 0$ if the force is defined as in 3.1.1. If $\Delta r < 0$ then $F_w = 0$.

Bellow Force

To describe the force the air bellow exerts on the system an approach found in [8][6] is used and is presented in (3.16). A_{eff} corresponds to the effective area the pressure acts upon to produce the force F_{ab}. The pressure p_{ab} is the pressure inside of the air bellow and p_{amb} the ambient pressure which is assumed to be constant.

$$F_{ab} = (p_{ab} - p_{amb})A_{eff} \tag{3.16}$$

This equation raises the need to describe the two new variables A_{eff} and p_{in}. The effective area is hard to measure directly [6] and can instead be estimated through data describing the force exerted by the bellow depending on height and pressure. The corresponding data is supplied by Scania and the pressure is derived from thermodynamical relations described in Section 3.1.3.

Damper Force

A look-up table describing the force from the damper with respect to it's extension/compression velocity was found at Scania, therefore the damper force was not modeled with the help of the law's of physics. The look-up table is essentially a piecewise affine function with respect to its velocity. The data is described in Figure 3.5 [1].

3.1.3   Fluid-mechanics and Thermodynamics

Equation (3.16) raises the need to model the pressure in the bellow which depends on the air-flow in and out of the bellow. These variables are defined in this sub-section.
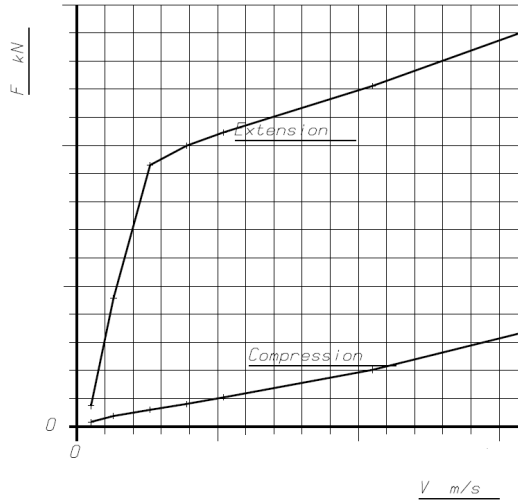
Figure 3.5: The look-up table used to describe the force from the damper.

Pressure

The pressure inside the bellow is calculated using the ideal-gas law described in
(3.17). This approach to model the pressure is also done in [11]. Here R is the
universal gas constant, T the temperature of the air inside the bellow in Kelvin,
V volume, p_{ab} the absolute pressure in the bellow and n number of air particals
inside the bellow.

$$p_{ab}V = nRT, \text{ or}$$
$$p_{ab} = \frac{nRT}{V}. \tag{3.17}$$

The volume is calculated with the average cross sectional area A of the bel-
low(note that this is not the same as the effective area A_{eff}) and the height of
the bellow, the temperature is assumed to be equal to the ambient temperature.
The average cross sectional area varies depending on the bellows height, why this
will also be a tuning parameter. When the control valve is closed, n is constant.
The variable n can be described as in (3.18), also using the ideal gas law. Here
a new variable f_{air} is introduced corresponding to the air flow and the index 0
corresponds to the variables initial value.

$$n(f_{air}(t)) = \frac{p_{in0}V_0}{RT_0} + \int_{t_0}^{t} f_{air}(t)\mathrm{d}t. \tag{3.18}$$

Air Flow

The goal is to find the air flowing through the valve when it is in one of it's two open states (flow in or flow out of bellow). For each of these two states of the valve, the used model must be parametrized. This because the air flows through different channels, depending on state, which leads to different flow resistances. The air flow is derived from Poiseuille's Law, which results in the air flow with respect to the pressure difference over the channel presented in (3.19). The parameters R_{flow1} and R_{flow2} are estimated from experimental data available at Scania.

$$
\begin{aligned}
f_{air} &= 0 & if\ u_{valve} &= 0 \\
f_{air} &= \frac{\Delta p}{R_{flow1}} & if\ u_{valve} &= 1 \\
f_{air} &= \frac{\Delta p}{R_{flow2}} & if\ u_{valve} &= 2
\end{aligned}
\tag{3.19}
$$

In (3.19) the control signal in u_{valve} is introduced which is defined in 2.2.1.

3.2 Statistical Estimation

As mentioned in the beginning of this chapter a statistical approach is used to model the behaviour of the system and is further explained in this section.

3.2.1 Black-Box

Black-box modeling is useful to describe the input/output relation of a system or a part of a system, without knowing the underlying physical properties. The relation is instead described through predefined equations, typically differential equations. There are two main methods for black-box modeling:

- **Non-parametric** models are usually defined through methods such as frequency analysis, step response characteristics or impulse reponse characteristics.

- **Parametric** models are pre-defined model structures where the parameters are fitted to the data.

According to [7] non-parametric models are not applicable for closed systems and therefore not suitable for this thesis's system. Instead the focus in this thesis is parametric modeling.

Modeling the whole system as a black-box model would require a high quantity of estimation and validation data, an amount that is not feasible for this thesis. In [14] it is said that air suspensions are in general highly non-linear due to air compressibility and the airflow through the solenoid. Although, some parts of the system are more or less linear why linear black-box models are of interest and were one of the methods that are used to model the air suspension.

3.2.2   Linear Black-Box Models

A parametric black-box model is a predefined transfer function. The transfer functions can be built up in differen ways and in [7] four different models are presented which are summarized under this subsection.

General Structure

The general structure in (3.20) is given in [7] and is stated in discrete time. This is the most common approach, as the data usually is collected in discrete form.

$$y[t] = n[t] + w[t] \tag{3.20}$$

Here $w[t]$ is a disturbance term and $n[t]$ the noise-free output of the system. The last term can be written as

$$n[t] = G(p, \theta)u[t], \tag{3.21}$$

where $u[t]$ is the input signal and $G(q)$ is the transfer function, q the shift-operator and θ a vector of parameters. $G(q, \theta)$ is defined as

$$G(q, \theta) = \frac{B(q)}{F(q)} = \frac{b_1 q^{-n_k} b_2 q^{-n_k-1} + ... + b_{n_b} q^{-n_k-n_b+1}}{1 + f_1 q^{-1} + ... + f_{n_f} q^{-n_f}}. \tag{3.22}$$

The disturbance term $w[t]$ is defined in a similar way,

$$w[t] = H(q, \theta)e[t] \tag{3.23}$$

the variable $e[t]$ is white noise and $H(p, \theta)$ the transfer function which is defined as

$$H(q, \theta) = \frac{C(q)}{D(q)} = \frac{1 + c_1 q^{-1} c_2 q^{-2} + ... + c_{n_c} q^{-n_c}}{1 + d_1 q^{-1} + ... + d_{n_d} q^{-n_d}}. \tag{3.24}$$

If the equations (3.21), (3.23) and (3.20) are put together the model can be summarized as

$$y[t] = G(q, \theta)u(t) + H(q, \theta)e(t). \tag{3.25}$$

The parameter vector θ contains the constants b_i, f_i, c_i and d_i. The structure of the model in (3.25) is described by the so called structural parameters n_b, n_f, n_c and n_d, which describes the order of the model and n_k that describes the time delay.

ARX, ARMAX, BJ, OE

In [7] the four most common model structures ARX, ARMAX, BJ and OE are presented. These four models differ in how they handle the disturbance signal. The most general of these four is the BJ-model which corresponds to the derived equation (3.25). The model structure OE-model does not model the disturbance signal, i.e $H(q) = 1$, and is therefore described as

$$y[t] = \frac{B(q)}{F(q)} u[t] + e[t]. \tag{3.26}$$

In the model ARMAX the input signal and disturbance signal shares the same denominator, i.e. $F(q) = D(q) = A(q)$, which gives the following relations

$$A(q)y[t] = B(q)u[t] + C(q)e[t]. \tag{3.27}$$

The common model ARX is a simplified version of ARMAX with $C(q) = 1$, therefore given by

$$A(q)y[t] = B(q)u[t] + e[t]. \tag{3.28}$$

3.2.3 Grey-Box

When a physical model is derived it is not uncommon that not all parameters are known. These parameters can be estimated through collected data and solving the equation in (3.30). [7]

3.3   Estimation of Parameters

Now that the structure of the models are presented, a method for estimating their parameters is needed. There is a general methodology which is common for all types of models (linear, non-linear, regression, etc..). But depending on the type of model, different methods for solving the different steps of the method are used. This methodology is given in [7] and is summarized in the following paragraphs.

The idea is to minimize a loss function with respect to the parameter vector. This loss function needs a set of input/output data. In [7] a quadratic loss function is presented as

$$V(\theta) = \frac{1}{N} \sum_{k=1}^{N} \|y(t_k) - \hat{y}(t_k|\theta)\|^2. \tag{3.29}$$

Here, N is the amount of samples, θ the parameter vector, $y(t_k)$ the measured output and $\hat{y}(t_k|\theta)$ the predicted output. Now the loss-function shall be minimized with respect to θ giving the optimized parameter vector $\hat{\theta}_N$ as follows

$$\hat{\theta}_N = \underset{\theta}{\operatorname{argmin}}\, V(\theta). \tag{3.30}$$

When $V(\theta)$ is quadratic and the predictons are linear in the parameter, as in the ARX case, optimization problem (3.30), it's solution is a least-squares estimate of θ. As the problem in this thesis is solved with functions provided by the `Identification toolbox` in MATLAB, the solution is not derived in this report but briefly explained.

   For a linear-regression model the equation (3.30) can be solved algebraically through the least-square-method. The solution is derived in [7]. If the regression model is defined as

$$\hat{y}(t|\theta) = \theta^T \rho(t), \tag{3.31}$$

where $\rho(t)$ is the regressor containing old measurements and inputs, then the solution is

$$\hat{\theta}_N = \frac{1}{N^2} \sum_{t=1}^{N} \rho(t)y(t) \sum_{t=1}^{N} \rho(t)\rho(t)^T \tag{3.32}$$

if $\sum_{t=1}^{N} \rho(t)\rho(t)^T$ is positive-definite. With a more complex loss function, numerical optimization is employed to find $\hat{\theta}$.

3.4   Model Validation

When the model is computed it needs to be validated. By validating the model the quality of the model can be determined. To avoid over-fitting the model to the estimation data, the models are validated with as different data as possible. In the subsections below the validation methods used in this thesis are described.

3.4.1   NRMSE

Through out the thesis normalized root-mean-square error (NRMSE) is presented in percentage to validate the model's ability to accurately estimate the system's static output as well as dynamics, although a static error is better seen in this quantity.

$$NRMSE = 100(1 - \frac{\|y - \hat{y}\|}{\|y - mean(y)\|}) \tag{3.33}$$

3.4.2   Residual Analysis

Ideally the output error should not be correlated with the input signal. A correlation between the output error and the input indicates that not all of the system's dynamics are captured by the model. This can be determined by studying the residual, or prediction error,

$$\varepsilon(t) = y(t) - \hat{y}(t|\hat{\theta}). \tag{3.34}$$

The correlation function is given by

$$\hat{R}_{\varepsilon u}(\tau) = \frac{1}{N} \sum_{t=1}^{N} \varepsilon(t + \tau)u(t) \tag{3.35}$$

and should be close to zero. [7]

If the output error and the input signal really is non correlated, then (3.35) is approximately normally distributed for big N with an average of zero and a variance according to

$$P_r = \frac{1}{N} \sum_{k=-\infty}^{\infty} R_{\varepsilon}(k)R_u(k). \tag{3.36}$$

Here R_ϵ and R_u represent the residual's and input's covariance function. When presenting $\hat{R}_{\epsilon u}$ the lines $+/-\sqrt{P_r}$ are commonly plotted. If the correlation function is outside of this area, it is probable that there is a correlation between the residual an input signal.[7]

4

Proposed Model Structures

Four different models of the complete system are developed with the help from the sub-models described in Section 3. Three of them are models based on the two methods QCM 1 and QCM 2. The fourth is a combination of the stated models in 3.1.3 and an estimated OE-model. The models are presented below.

4.1 Model 1

The first model is based on QCM 1 where the forces are defined by (3.15) and (3.16), the pressure by equation (3.17) and air flow according to equation (3.19).

These combined gives the state-space model in (4.1), where x_1 and x_2 corresponds to the variables in Figure 3.2. The output y_1 is the bellow height and y_2 the absolute pressure in the air bellow.

$$\begin{aligned}
\dot{x}_1 &= x_3 \\
\dot{x}_2 &= x_4 \\
\dot{x}_3 &= \frac{k_l F_{ab}(x_1, x_2, x_5) - F_d(x_3, x_4) - m_1 g - (x_3 - x_4)k_f}{m_1} \\
\dot{x}_4 &= \frac{-k_l F_{ab}(x_1, x_2, x_5) + F_d(x_3, x_4) - F_w(x_2) - m_2 g}{m_2} \\
\dot{x}_5 &= f_{air}(x_1, x_2, u) \\
y_1 &= x_1 - x_2 \\
y_2 &= p_{in}(x_5, x_1, x_2)
\end{aligned} \tag{4.1}$$

4.2   Model 2

The second model is as Model 1 based on the sub-models presented in 3.1, but instead the kinematics are described with QCM 2 in equation (3.12). Also an extended version of this model is built to capture the slow dynamics seen in Figure 5.4.

   The nonextended model results in the nonlinear state-space presented below, where x_1 corresponds to α and x_2 to x in Figure 3.3.

$$
\begin{aligned}
\dot{x}_1 &= x_3 \\
\dot{x}_2 &= x_4 \\
\dot{x}_3 &= \frac{l_1 cos(x_1)(m_2 g - F_w(x_1, x_2)) + (l_1 + l_3)F_d(x_3)}{I_g} + \\
&\quad \frac{(l_1 + l_2)F_{ab}(x_1, x_5) - m_2 r_{Ag} a_{g\perp}(x_1, x_3, \ddot{x})}{I_g} \\
\dot{x}_4 &= \ddot{x} = \frac{F_w(x_1, x_2) - (m_1 + m_2)g}{m_1 + m_2} \\
\dot{x}_5 &= f_{air}(x_5, x_1, u) \\
y_1 &= h_{QCM2}(x_1) \\
y_2 &= p_{in}(x_1, x_5)
\end{aligned}
\tag{4.2}
$$

4.2.1   Model 2 - Extended

The extended version uses a linear statistical model to describe the slow dynamics seen in 5.1.2, which has the mass as input and an extra term added to the bellow force as output. The OE model by itself is represented, when converted to a continous-time state-space model using the method "Zero-Order-Hold", as

$$
\begin{aligned}
\begin{pmatrix} \dot{x}_1 \\ \vdots \\ \dot{x}_n \end{pmatrix} &= \begin{pmatrix} A_{11} & \dots & A_{1n} \\ \vdots & \ddots & \vdots \\ A_{n1} & \dots & A_{nn} \end{pmatrix} \begin{pmatrix} x_1 \\ \vdots \\ x_n \end{pmatrix} + Bm_2 \\
F_{ext} &= \begin{pmatrix} C_1 & \dots & C_n \end{pmatrix} \begin{pmatrix} x_1 \\ \vdots \\ x_n \end{pmatrix} + Dm_2.
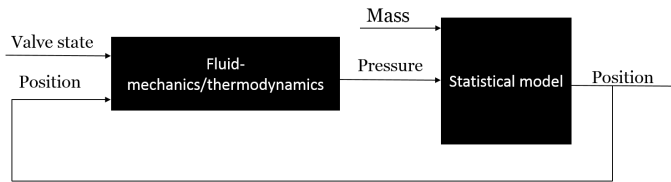\end{aligned}
\tag{4.3}
$$

Here, n represent the number of states. Note that the noise signal e(t) is not present, as it is not of interest to model the noise and therefore was set to zero.

Combined with the nonlinear state-space stated in (4.2) gives

$$y_1 = h_{QCM2}(x_1)$$
$$y_2 = p_{in}(x_1, x_5)$$
$$\dot{x}_1 = x_3$$
$$\dot{x}_2 = x_4$$
$$\dot{x}_3 = \frac{l_1 \cos(x_1)(m_2 g - F_w(x_1, x_2)) + (l_1 + l_3)F_d(x_3)}{I_g} +$$
$$\frac{(l_1 + l_2)(F_{ab}(x_1, x_5) + F_{ext}) - m_2 r_{Ag} a_{g\perp}(x_1, x_3, \ddot{x})}{I_g}$$
$$\dot{x}_4 = \ddot{x} = \frac{F_w(x_1, x_2) - (m_1 + m_2)g}{m_1 + m_2} \qquad (4.4)$$
$$\dot{x}_5 = f_{air}(x_5, x_1, u)$$
$$\dot{x}_6 = A(1,:)x_6 + Bm_2$$
$$\vdots$$
$$\dot{x}_{n+5} = A(n,:)x_{n+5} + Bm_2$$
$$F_{ext} = \begin{pmatrix} C_1 & \cdots & C_n \end{pmatrix} \begin{pmatrix} x_6 \\ \vdots \\ x_{n+5} \end{pmatrix} + Dm_2.$$

4.3   Model 3

The third model created is a combination between the sub-models that describes the pressure and a linear statistical model, as presented in 3.2.2.

Figure 4.1: *Block scheme describing the relations between the different input and output signals.*

In Figure 4.1 the model is represented as a block-diagram. Furthermore, the model's nonlinear state-space is represented by

$$
y_1 = h_{bellow} = \begin{pmatrix} C_1 & \dots & C_n \end{pmatrix} \begin{pmatrix} x_2 \\ \vdots \\ x_n \end{pmatrix} + D \begin{pmatrix} m_2 \\ p_{in}(x_1, h_{bellow}) \end{pmatrix}
$$

$$
y_2 = p_{in}(x_1, h_{bellow})
$$
$$
\dot{x}_1 = f_{air}(x_1, h_{bellow}, u)
$$
$$
\dot{x}_2 = A(1,:)x_2 + B(1,:) \begin{pmatrix} m_2 \\ p_{in}(x_1, h_{bellow}) \end{pmatrix}
$$

$$
\vdots
$$

$$
\dot{x}_{n+1} = A(n,:)x_{n+1} + B(n,:) \begin{pmatrix} m_2 \\ p_{in}(x_1, h_{bellow}) \end{pmatrix},
$$

$$(4.5)$$

where the statistical model is converted to a continous-time state-space model using "Zero-Order-Hold" method and n describes the number of states.

5

Parameter Estimation and Model Validation

5.1 Collection of Data

Under this section it is explained how the data is collected and under what circumstances. Also the data that is used to estimate and validate the model is presented. The collected data sets will be refereed to as data-set 1-4.

5.1.1 Test Environment

Data collection is done on a truck provided by Scania. It is a 4x2 (2 axles, 1 drive axle) long haulage truck with an air suspension at the rear (drive) axle, identical to the suspension shown in Figure 2.1. The height and pressure of one bellow is of interest, more specifically the left bellow because of the location of the height and pressure sensors.

To know how the weight is distributed over the four wheels, the weight put on each wheel is measured through individual scales under each wheel. Unfortunately, the measured weight had to be manually noted through a display showing the weight put on each wheel.

The signals that were measured are:

- Height (through pre-installed height sensor)

- Height (through calibrated height sensor)

- Pressure in bellow

- State of valve

- Pressure in actuator tank

5.1.2 Steps in Load

Data is collected when steps in the load are made. The steps in the load are produced with the help of a traverse which pulls up or lowers down weights of one ton on/off the truck. This is done as quickly as possible to approximate a step-response, which is not optimal, firstly because the step is not as fast as the approximated load signals steps. Secondly how fast the different steps are done vary and sometimes complications occurred, especially when loading on weights.

Two sets of data are collected for the purpose of having both estimation and validation data. To become a difference in the two data sets, the weights are lifted on/off in different orders. In Figure 5.1 and Figure 5.2 the estimation data is presented, from now on referred to as data-set 1. Here the sprung mass refers to the weight that the scale showed at one wheel, subtracted with half of the weight of the axle and one wheel.
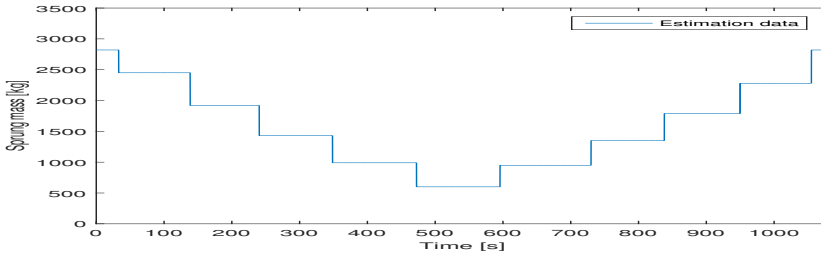
Figure 5.1: Estimation data (data-set 1), sprung mass.

Analyzing the behaviour in the estimation data plots and specifically the height, first an expected fast dynamic can be seen followed by a slower, less expected, dynamic. In Figure 5.3 and Figure 5.4 the validation data set is presented, from now on refereed to as data-set 2.

Collecting the validation data, there were more complications with the loading than with the estimation data, for example seen between 950 and 1000 seconds in Figure 5.4. This is the main reason why this data set was chosen to be the validation data.

5.1.3 Steps In Air Flow

To validate the model's behaviour when the valve is opened or closed two data sets are collected. One (data-set 3) where several shorter steps in the control signal are done, both filling and exhausting the bellow, is presented in Figure 5.5. The other data set (data-set 4), longer steps in the control signal are provided. This data is presented in Figure 5.6. Throughout the procedure the load was constant at a sprung mass of 2830 kg.
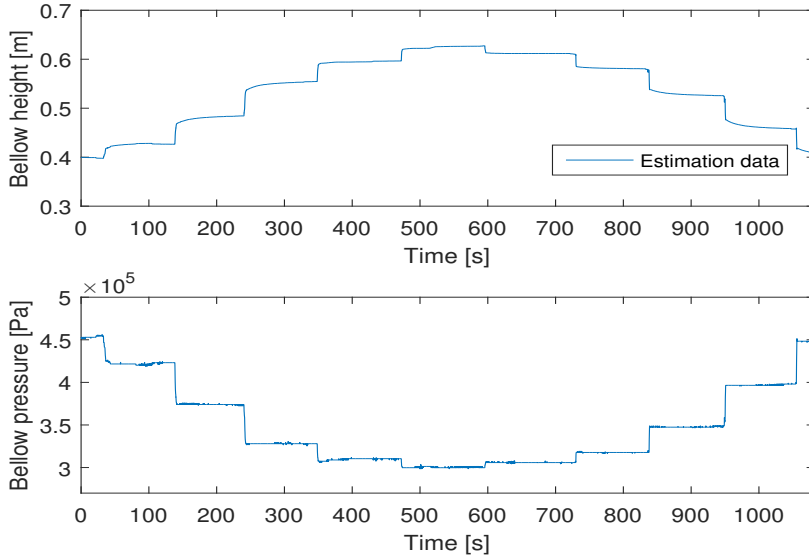
Figure 5.2: Collected estimation data (data-set 1), height and pressure.
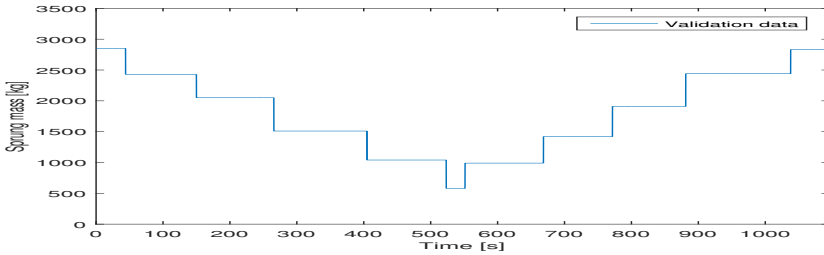
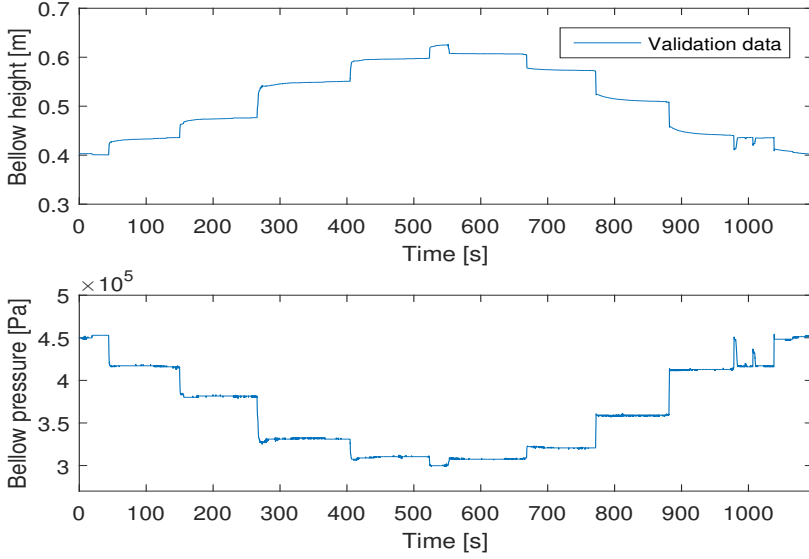*Figure 5.3: Validation data (data-set 2), sprung mass.*

5.2   Parameter Estimation

Some of the system's parameters are hard to measure or do not directly translate to the model's parameters and must therefore be estimated, as well as the statistical model's parameters must be estimated. Under this section it is explained how the parameters are estimated to fit the collected or given data.

5.2.1   Cross Sectional Area

As mentioned before the cross sectional area varies with the height of the bellow. The cross sectional area is approximated with a linear function,

$$A(h_{bellow}) = A_0 + A_1 h_{bellow} \tag{5.1}$$

Figure 5.4: Collected validation data (data-set 2), height and pressure.

and the parameters A_0 and A_1 are estimated by solving the optimization function

$$\hat{A}(h_{bellow}) = \underset{A_0, A_1}{\operatorname{argmin}}(p(h_{bellow}) - \hat{p}(A(h_{bellow}))), \tag{5.2}$$

where $\hat{p}(A(h_{bellow}))$ is defined as

$$\hat{p}(A(h_{bellow})) = (p(h_{bellow}) - \frac{nRT}{h_{bellow}A(h_{bellow})}). \tag{5.3}$$

Here $\hat{p}(A(h_{bellow}))$ is the estimated bellow pressure with height from data-set 1, where the the valve is closed through out the experiment. The function that is minimized is nonlinear and complex, $A(h_{bellow})$ is therefore found through numerical methods. The resulting parameters are shown in Table 5.1 together with the respective NRMSE values for the pressure model.

A_0	A_1	NRMSE Estimation data	NRMSE Validation data
0.250	-0.0310	90.85%	92.19%

Table 5.1: *Parameter values for cross sectional area linear function and NRMSE values for pressure model.*

5.2.2   Effective Area

The effective area with respect to the bellow's height is found through applying the least-square-method presented in 3.3 to the equation (3.16) describing the
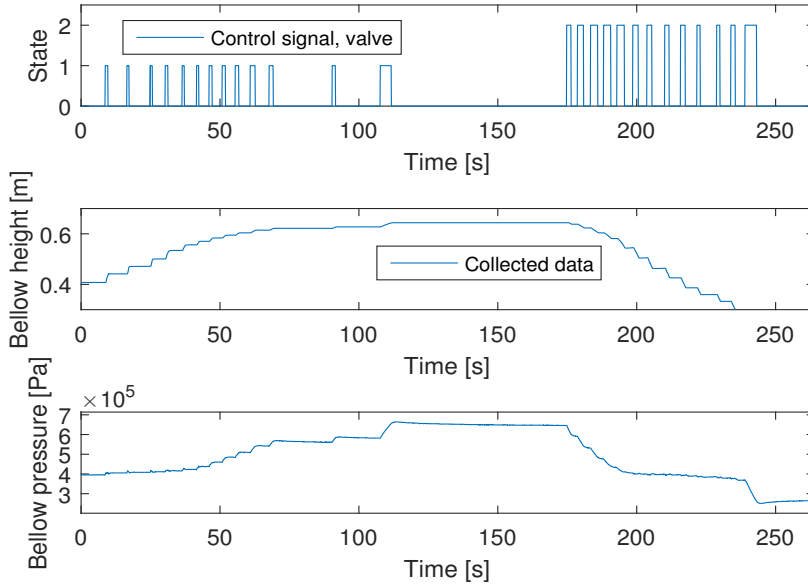
Figure 5.5: *Collected data when filling and exhausting the air bellow in shorter steps (data-set 3).*

bellow force w.r.t. to the pressure. From this a vector describing the effective area w.r.t. the bellows height is given, which then is fitted to a polynomial of fourth degree.

$$A_{eff}(h_{bellow}) = p_0 + p_1 h_{bellow} + p_2 h_{bellow}^2 + p_3 h_{bellow}^3 + p_4 h_{bellow}^4 \qquad (5.4)$$

with the corresponding estimated parameters presented in Table 5.2 Although

p_0	p_1	p_2	p_3	p_4
-0.0289	0.08362	-3.0698	4.9616	-2.9941

Table 5.2: *The estimated parameters for the polynomial function describing the effective area of the air bellow.*

no validation data is available, it is of interest to see how well the polynomial function is fitted to the estimation data. In Figure 5.8 the estimation data can be seen, as well as how good the polynomial function fits to the estimation data.

A problem that the data presents, is that the data is collected in a lab-environment where the air bellow was compressed and extended in a vertical manner. This does not fully represent the true system, where the bellow compresses and extends in a circular manner due to how it is installed. To further fit the parameters
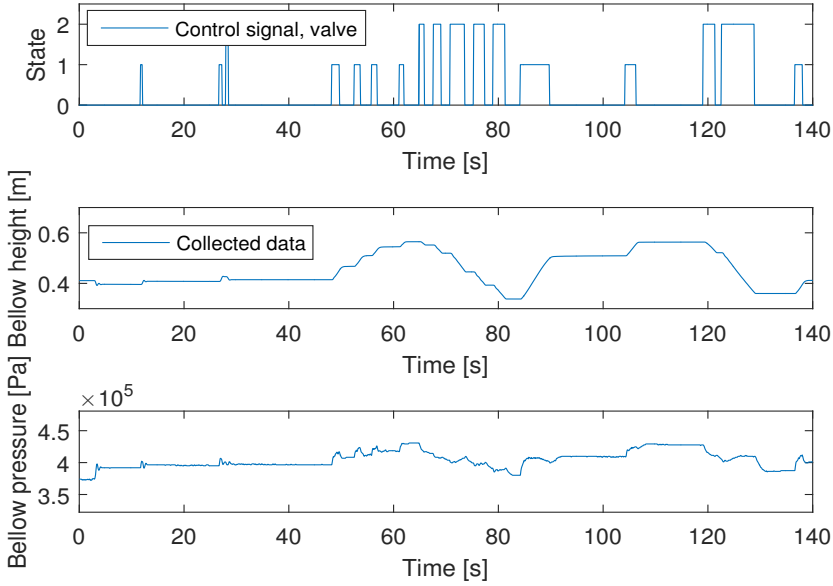
Figure 5.6: *Collected data when filling and exhausting the air bellow in longer steps (data-set 4).*

to the system, the parameters in Table 5.2 are further estimated when applied to the model using the Grey-Box method described in 3.2.3.

5.2.3   Air Flow

To estimate the constant R_{flow} and the parameters of the polynomial function found in equation (3.19), data collected at Scania is used. The data is collected through measuring the pressure of a tank filled with compressed air connected to the valve and letting the air out in the atmosphere, either through the exhaust channel or the inlet channel of the valve. Two data-sets for both filling and exhaust are collected, providing both estimation and validation data. The two data sets are collected with the same experiment setup, why the validation data can be questioned to be too similar to the estimation data.

   The air flow was not directly measured and thus has to be derived from the measured pressure and the ideal gas law

$$n = \frac{p_{tank} V_{tank}}{RT}, \tag{5.5}$$

where R is the earlier mentioned gas constant, T was approximated to be equal to normal room temperature and V_{tank} is volume of the tank. The derivative of n with respect to time then gives the air flow as follows
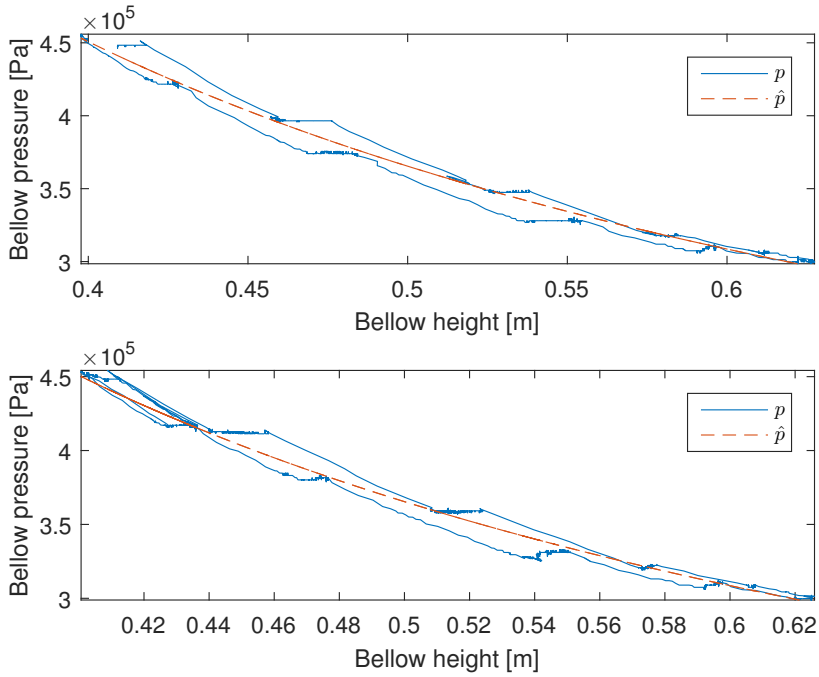
Figure 5.7: *Pressure w.r.t. the bellows height, estimation (top plot) and validation (bottom plot) data (data set 1 and 2 resp.) as well as the estimated pressure using the model.*

$$\frac{dn}{dt} = \frac{dp}{dt}\frac{V_{tank}}{RT}.$$ (5.6)

The derivative of the the pressure is estimated numerically from the data that is collected. The outcome when equation (5.6) is applied to the data is presented in Figure 5.9.

To estimate the constant for both filling and exhaust (R_{flow1} & R_{flow2}), the least-square-method described in 3.3 is applied to equation (3.19).

In Table 5.3 the NRMSE values for the air-flow model is presented.

	NRMSE
Filling	64.06 %
Exhaust	62.77 %

Table 5.3: *The NRSME-values for the air flow submodel compared to validation data with equation (5.6) applied.*

The submodel is compared to the data in Figure 5.10 - 5.13.
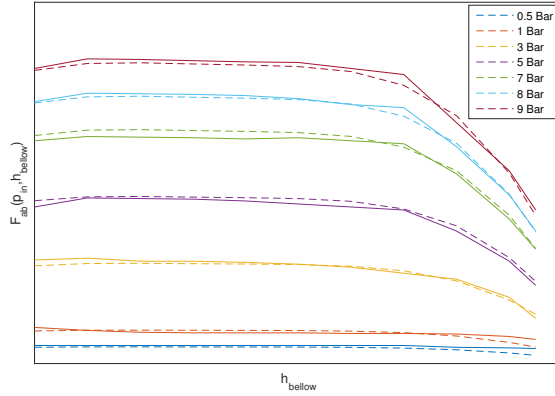
Figure 5.8: *Graph showing the static data (line) representing the load depending on height where each line represents different relative pressures for the air bellow. The dotted line is the estimated force w.r.t. bellow height and pressure.*
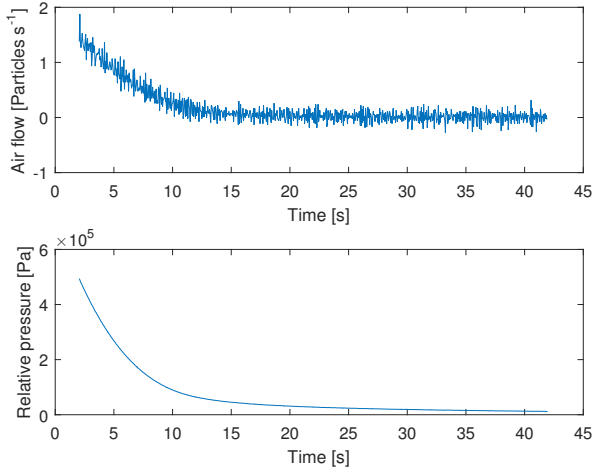
Figure 5.9: *Upper graph showing the air flow at the top and lower graph the pressure in the tank, when exhaust channel open.*

### 5.2.4   Linear Statistical Model Describing Slow Dynamics

When estimating the linear statistical model for Extended Model 2, the slow dynamics in one step is isolated. Resulting in the mass being the input and the height the output. The static relation is removed, meaning that the initial values of the input and output signal are zero. The output that is wished to be mod-
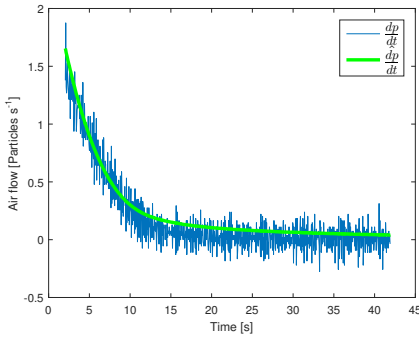
Figure 5.10: *Air flow submodel compared to the estimation data when filling.*
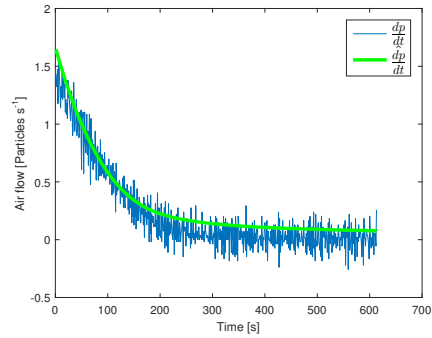
Figure 5.11: *Air flow submodel compared to the validation data when filling.*
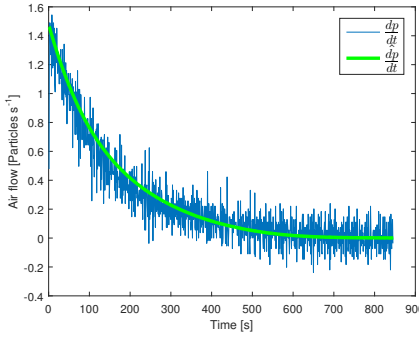
Figure 5.12: *Air flow submodel compared to the estimation data when exhaust.*
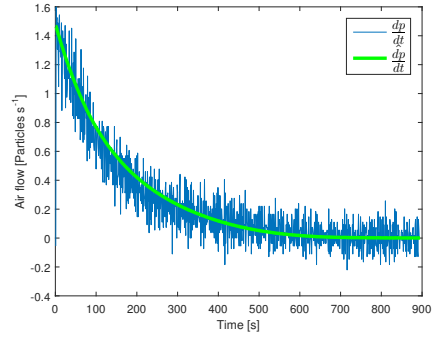
Figure 5.13: *Air flow submodel compared to the validation data when exhaust.*

eled is the force from the bellow, which is not possible to do directly as the force could not be measured. Instead the relation between the height and the force is assumed to be proportional. This results in a proportionality parameter k_{sd} that is first manually estimated as approximately one tenth of the the force from the bellow at a certain height. The parameter is then further estimated in 5.2.6 with the help of the Greybox-method described in 3.2.3.

To find a suitable statistical model describing the slow dynamics of the system, several model structures are tested and evaluated using the `Identification Toolbox` in MATLAB resulting in a OE-model with the parameter structure as presented in Table 5.4. The order is chosen so that the model estimates the output sufficiently well, but without estimating any possible disturbance created from experiment errors. As the input signal is manually constructed, the time delay chosen might not correspond to the time delay of the true system. Furthermore,

it is a simple dynamic not requiring a high order model structure. The order chosen is presented in Table 5.4.

	n_b	n_f	n_k
OE-Model	1	1	2

Table 5.4: *The selected model order parameters for the OE-model.*

The estimated parameters are given in Table 5.5 resulting in a NRSME-value of 95.8%, when compared to the estimation data.

Parameter	Value	Standard deviation
b_1	$-8.672 * 10^{-8}$	$\pm 3.327 * 10^{-10}$
f_1	-0.997	$\pm 1.41 * 10^{-5}$

Table 5.5: *The estimated parameter values and their standard deviation, for the OE-model.*

5.2.5   Model 3 - Statistical Model

The third proposed model structure, Model 3, uses a statistical model to explain the relation between the input pressure, mass and output bellow height. The model structure OE is used and the order of the model is presented in 5.6. The order is chosen through iterative search for the optimal solution and also considering not over-fitting the model, the resulting order is given in Table 5.6. The

	n_b	n_f	n_k
OE-Model	[2 2]	[2 2]	[1 1]

Table 5.6: *The model order parameters for proposed Model 3.*

resulting parameters are given in Table 5.7 and 5.8, which are estimated from data-set 1. The parameters are estimated using `Identification Toolbox` with simulation focus, providing with a stable model with it's poles inside the of the unit-circle.

Parameter	Value	Standard deviation
b_1	$1.093 * 10^{-5}$	$\pm 7.116 * 10^{-7}$
b_2	$1.093 * 10^{-5}$	$\pm 7.115 * 10^{-7}$
f_1	-1.84	± 0.01075
f_2	0.8404	± 0.01075

Table 5.7: *The parameter values of the estimated OE-model for mass input, for proposed Model 3.*

Parameter	Value	Standard deviation
b_1	$-5.801 * 10^{-9}$	$\pm 1.725 * 10^{-9}$
b_2	$5.194 * 10^{-9}$	$\pm 1.685 * 10^{-9}$
f_1	-0.5059	± 0.2309
f_2	0.4933	± 0.231

Table 5.8: *The parameter values of the estimated OE-model for pressure input, for proposed Model 3.*

5.2.6 Greybox Estimation

Certain parameters are estimated through greybox estimation, theory presented in 3.2.3. Different combinations of parameters are estimated at the same time. The NRMSE-value is presented for each model compared with the estimation data. These estimations are only done with data-set 1. The nominal NRMSE values in Table 5.10-Table 5.12 uses initial values, estimated or approximated as presented earlier in the report. How the initial values are chosen, is summarized in Table 5.9.

p_0, p_1, p_2, p_3, p_4	Defined in section 5.2.2 with least square method.
m_2	Total mass on wheel subtracted with wheel and half of axle weight.
k_f	Initial guess of 0.1.
I_g	Defined in equation (3.8).
k_{sd}	One tenth of bellow force at initial conditions.

Table 5.9: *How the parameters that are further estimated with greybox method are initially approximated or estimated.*

Model 1

	Nominal	Estimation 1	Estimation 2	Estimation 3
Numerically optimized parameter(s)		p_0, p_1, p_2, p_3, p_4	p_0, p_1, p_2, p_3, p_4 m_2 k_f	m_2 k_f
Height NRMSE	-21.02 %	82.93 %	82.88 %	9.84 %
Pressure NRMSE	6.646 %	88.00 %	88.01 %	91.42 %

Table 5.10: *Parameters estimated with greybox and the resulting NRMSE-values for simulation results compared to data for Model 1.*

The negative result shown for the nominal parameters in 5.10 are caused due to the second norm of the difference between the measured and simulated signal is larger than the second norm of the difference between the measured signal and its average value.

Model 2 - Nonextended

	Nominal	Estimation 1	Estimation 2	Estimation 3
Numerically optimized parameter(s)		p_0, p_1, p_2, p_3, p_4	p_0, p_1, p_2, p_3, p_4 m_2 I_g	m_2 I_g
Height NRMSE	65.18 %	83.56 %	88.19 %	64.89 %
Pressure NRMSE	65.77 %	88.65 %	90.97 %	68.32 %

Table 5.11: *Parameters estimated with greybox and the resulting NRMSE-values for simulation results compared to data for nonextended Model 2.*

Model 2 - Extended

	Nominal	Estimation 1	Estimation 2	Estimation 3
Numerically optimized parameter(s)		p_0, p_1, p_2, p_3, p_4	p_0, p_1, p_2, p_3, p_4 m_2 I_g k_{sd}	m_2 I_g k_{sd}
Height NRMSE	66.89 %	83.96 %	87.35 %	74.32 %
Pressure NRMSE	62.12 %	87.37 %	89.4 %	61.01 %

Table 5.12: *Parameters estimated with greybox and the resulting NRMSE-values for simulation results compared to data for extended Model 2.*

The statistical model present in the extended version of model 2 was separately estimated as described section 5.2.4.

5.3 Validation of Final Models

When validating the models, the best grey box parameter estimation according to the NRMSE values in 5.2.6 for proposed Model 1 and Model 2 are chosen to be further evaluated.

5.3.1 Model 1

According to the NRMSE values for each grey-box estimation for model 1, estimation 1 and 2 gives similar results. Estimation two is further evaluated under this subsection.

In Table 5.13 the NRMSE values for the validation data are presented. Higher NRMSE values are seen for data-set 2 then for data-set 3 and 4 in the table.

The main difference between the data sets, probably the reason for the large difference in results, are that data-set 2 only changes the mass and data-set 3-4 only changes the valve state and actuator pressure.

	data-set 2	data-set 3	data-set 4
NRMSE height	85.88 %	24.97 %	−43.46 %
NRMSE pressure	88.35 %	37.4 %	−255.1 %

Table 5.13: *NRMSE values for Model 1 when simulated with validation data.*

Validation of Model 1 with data-set 2

Seen in Figure 5.14 is the simulated response from Model 1 when input from data-set 2 is used. It captures the steps but fails to capture the slow dynamics seen in the measured data, and it overshoots during loading. In Figure 5.15 the residual analysis is plotted, showing that the cross correlation between the residuals and input have values outside of the area of 99 % confidence.
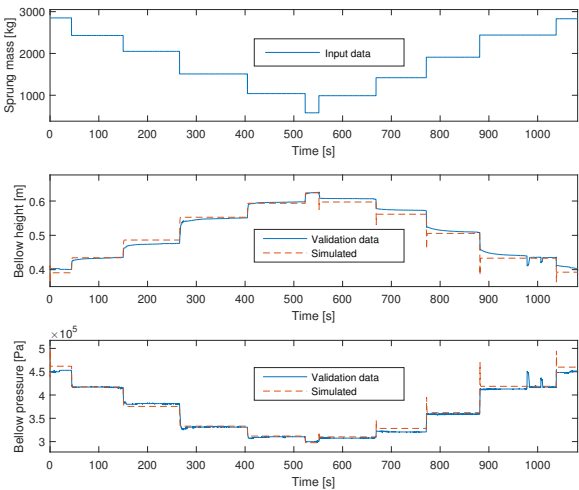
Figure 5.14: *Model 1 simulated and compared with data-set 2.*
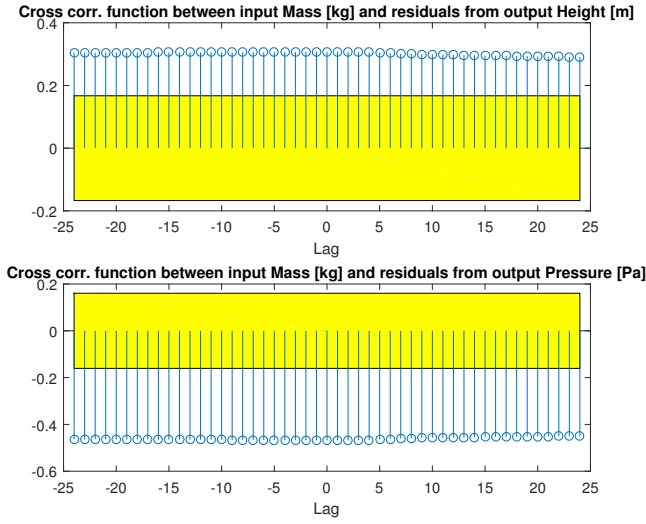
Figure 5.15: *Residual analysis for Model 1 with data-set 2, the yellow area is the 99 % confidence interval.*

Validation of Model 1 with data-set 3

In Figure 5.16 the result from the simulation of Model 1 together with data-set 3 is presented. It is seen that, first of all a initial offset in bellow pressure and height is seen and then the model fails to follow the validation data accurately. In Figures 5.17-5.20 the residual analysis of the model is presented. Model 1 do not indicate any correlation between the inputs and the pressures residual, although the error in height seems to correlate with the input signals.
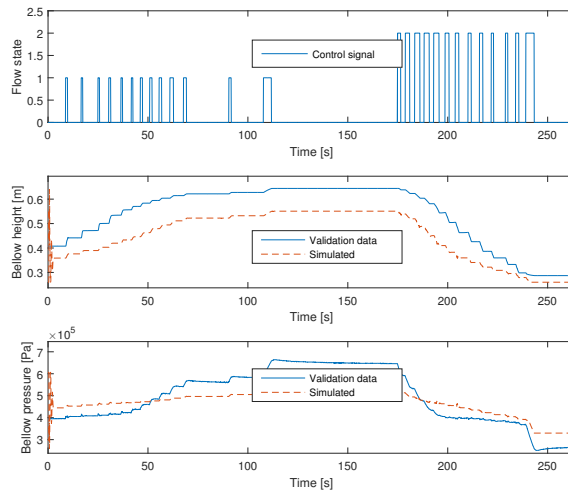
Figure 5.16: Model 1 simulated and compared with data-set 3.
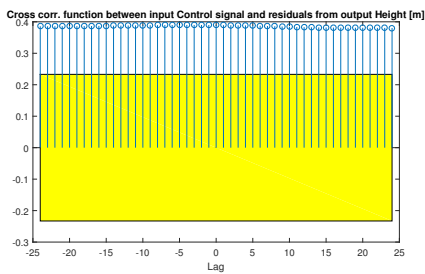
Figure 5.17: Cross correlation function for data-set 3 showing that there is correlation between the control signal and the the error in height.
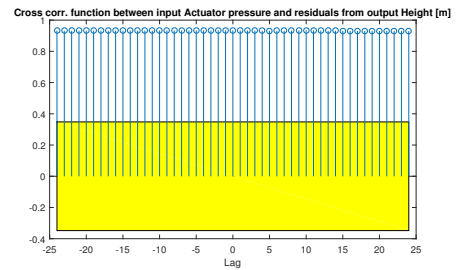
Figure 5.18: Cross correlation function for data-set 3 showing that there is correlation between the actuators tank pressure and the error in height.
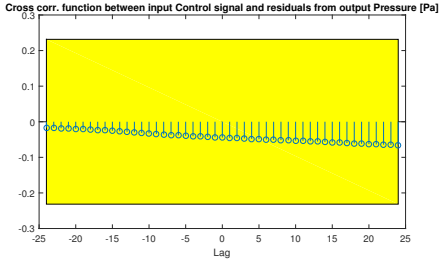
Figure 5.19: *The cross correlation function between the control signal and the error in pressure not indicating any correlation.*
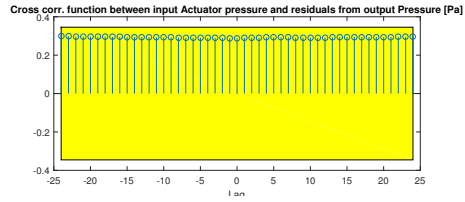
Figure 5.20: *The cross correlation function between the control signal and the error in pressure, just inside of the 99 % confidence interval.*

Validation of Model 1 with data-set 4

Looking at the simulation results, in Figure 5.21 from Model 1 with data-set 4, a similiar initial and continuing offset is seen as when simulated with data-set 3. Here the residual analysis, plotted in Figure 5.22 - 5.25, indicate more correlation between input and output-error than when simulated with data-set 3.
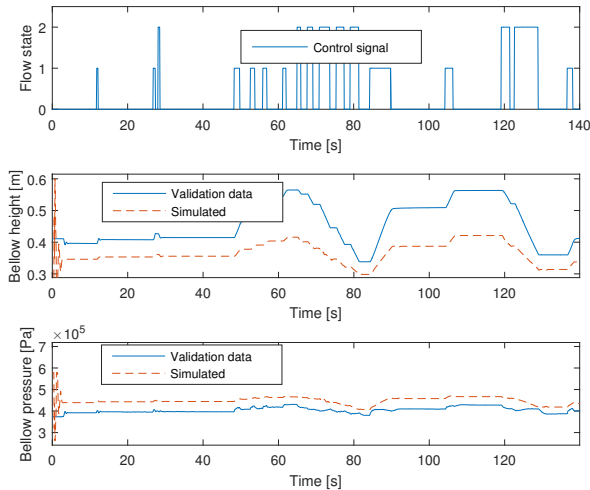
Figure 5.21: *Model 1 simulated and compared with data-set 4.*
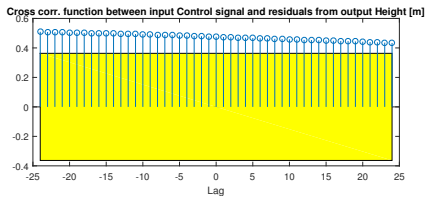
Figure 5.22: *Cross correlation between control input and height error, with values just outside the confidence interval.*
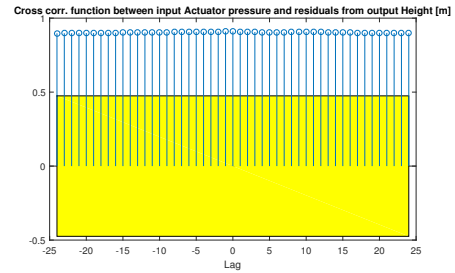
Figure 5.23: *Cross correlation between actuator tank pressure and height error, with values outside of the confidence interval.*
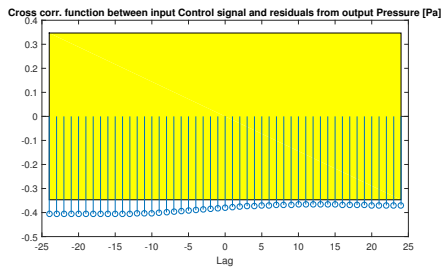
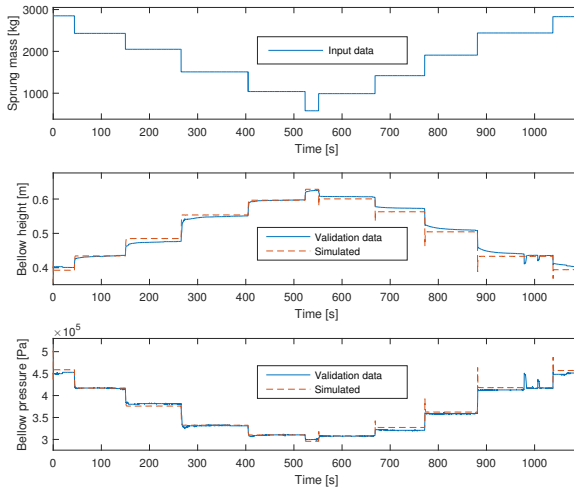**Figure 5.24:** *Cross correlation between control input and pressure error, with values just outside of the confidence interval.*
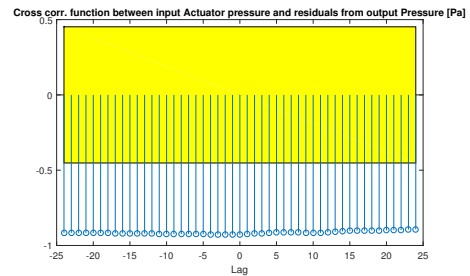
Figure 5.25: *Cross correlation between actuator tank pressure and height error, with values outside of the confidence interval.*

5.3.2   Model 2 Nonextended

For the nonextended version of model 2 estimation 2 (from Table 5.11) is chosen for further evaluation. In Figure 5.26 - 5.33 simulation with validation data is presented. The NRMSE values for each simulation is presented in Table 5.14.

	data-set 2	data-set 3	data-set 4
NRMSE height	86.88 %	31.37 %	−36.18 %
NRMSE pressure	89.74 %	35.7 %	−218.80 %

Table 5.14: *NRMSE values for nonextended Model 2 when simulated with validation data.*

Validation of Model 2 nonextended with data-set 2

Model 2 nonextended simulated respons together with data-set 2 is presented in
5.26 giving similar results as for Model 1. The residual analysis presented in Fig-
ure 5.27 indicates that there might be correlation between the pressure residual
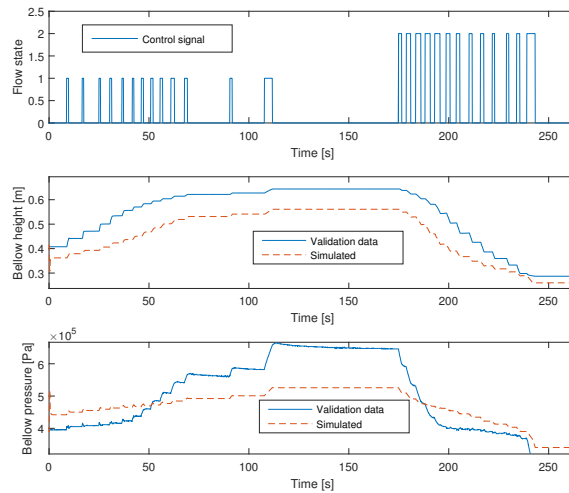and the mass input.

***Figure 5.26:*** *Model 2 nonextended simulated and compared with data-set 2.*
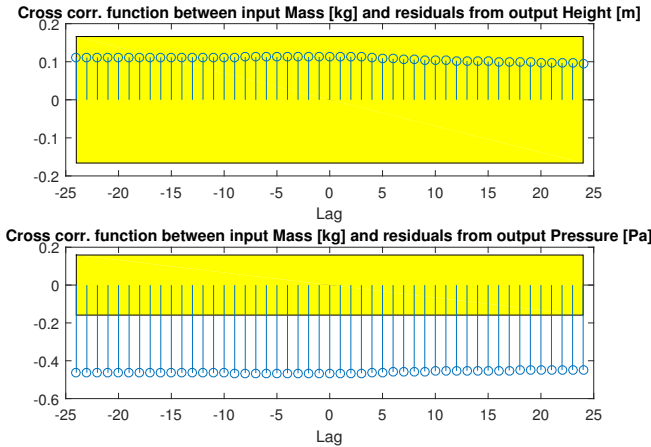
Figure 5.27: *Residual analysis for Model 2 nonextended with data-set 2. The
lower graph, showing the cross correlation between mass and error in simu-
lated pressure, indicates some correlation between residual and input.*

Validation of Model 2 nonextended with data-set 3

In Figure 5.28 the simulation results for Model 2 nonextended together with data-set 3 is shown. Similar problems occurs with the nonextended version of Model 2 as with Model 1, with an initial and continuing offset. The residualanalysis plots shown in Figure 5.29 - 5.32, as in Model 1, indicates high correlation between pressure in actuator tank and the height's residual.
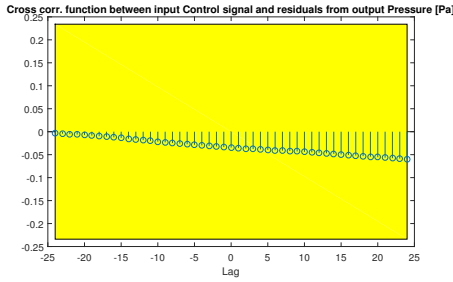

Figure 5.28: *Model 2 nonextended simulated and compared with data-set 3.*
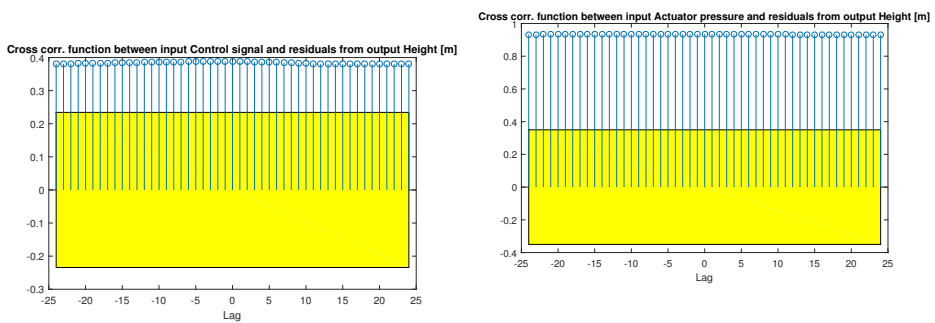
Figure 5.29: *Cross correlation plot indicating correlation between height residual and control signal.*

Figure 5.30: *Cross correlation plot indicating correlation between height residual and actuator pressure in tank with values far out from confidence interval.*
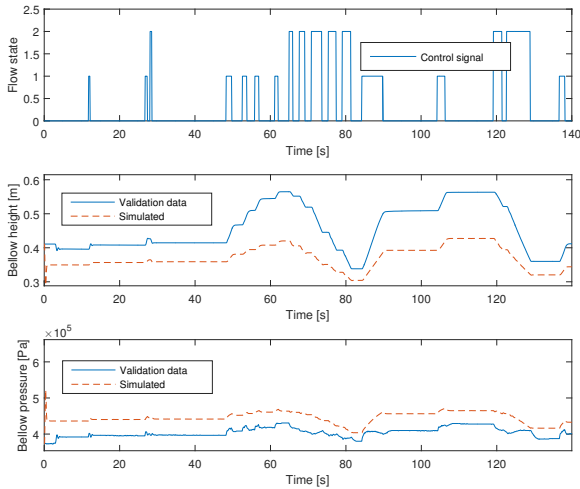
Figure 5.31: *Residual analysis indicating no correlation between control signal and pressure residual.*
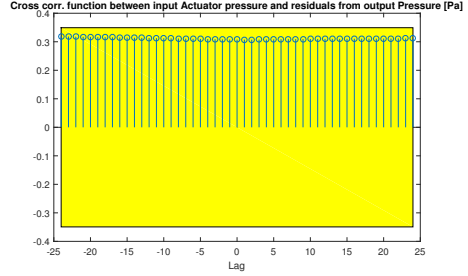
Figure 5.32: *Cross correlation function between pressure in actuator tank and the pressures residual, just inside of confidence interval.*

Validation of Model 2 nonextended with data-set 4

Similar results, shown in Figure 5.33, are presented when the nonextended Model 2 is simulated with data-set 4 as with data-set 3. The residual analysis indicates a strong correlation between actuator pressure and output residuals, seen in Figure 5.35. In Figure 5.34, 5.36 and 5.37 the remaining cross correlation functions are plotted.
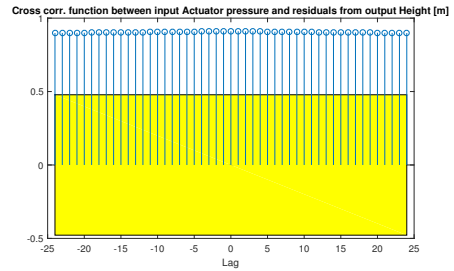

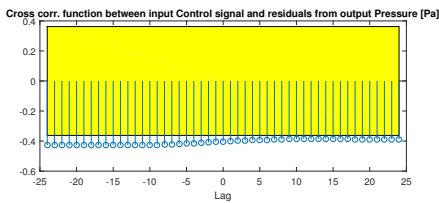**Figure 5.33:** *Model 2 nonextended simulated and compared with data-set 4.*
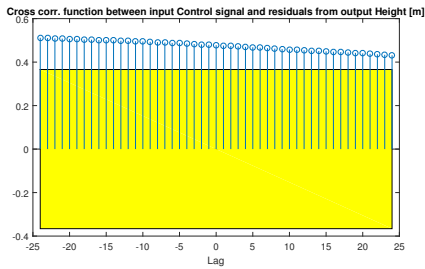
Figure 5.34: *Cross correlation function indicating some correlation between control signal and height residual.*

Figure 5.35: *Cross correlation between acutator pressure and height residual, showing strong correlation between the two.*

Figure 5.36: *Cross correlation between control signal and pressure residual.*
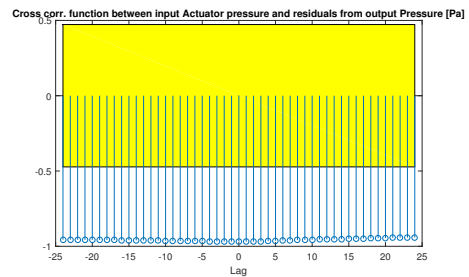
Figure 5.37: *Cross correlation between actuator pressure and residual from pressure, with values far outside the 99 % confidence interval.*
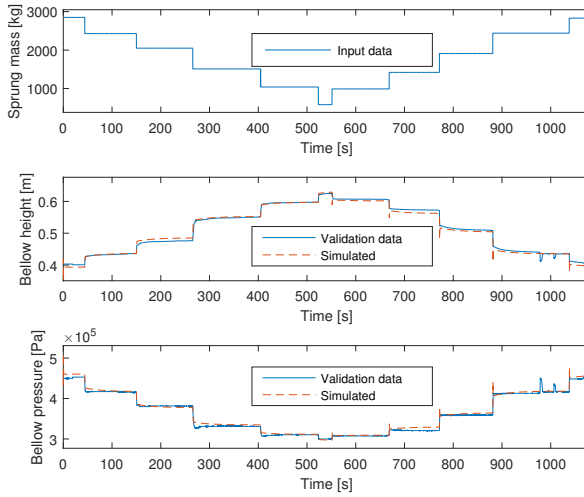
5.3.3   Model 2 Extended

Under this subsection the extended version of Model 2 is validated, using the same approach as in 5.3.1 and 5.3.2. The NRMSE values for the model when simulated with each set of data is presented in Table 5.15.

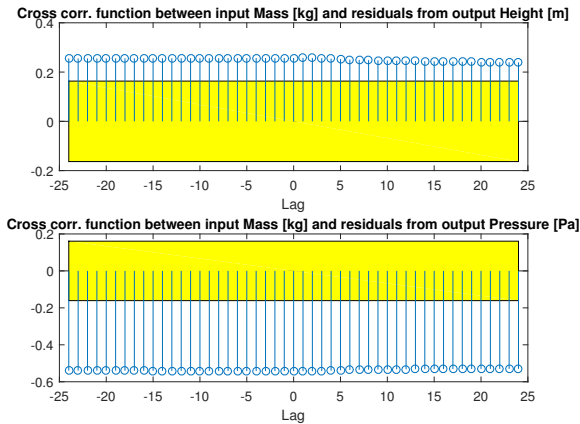|	data-set 2	data-set 3	data-set 4
NRMSE height	91.14 %	5.78 %	−34.61 %
NRMSE pressure	89.63 %	50.6 %	−210.7 %

Table 5.15: *NRMSE values for extended Model 2 when simulated with validation data.*

Validation of Model 2 extended with data-set 2

The output from the extended version of Model 2, shown in Figure 5.38, seems to capture the systems dynamics as well as the two earlier validated models, but with the addition of capturing the slower dynamics. The residual analysis, presented in Figure 5.39, it is seen that also this model presents correlation between the mass input and the residual of the outputs, although higher corrleation to the pressure residual.
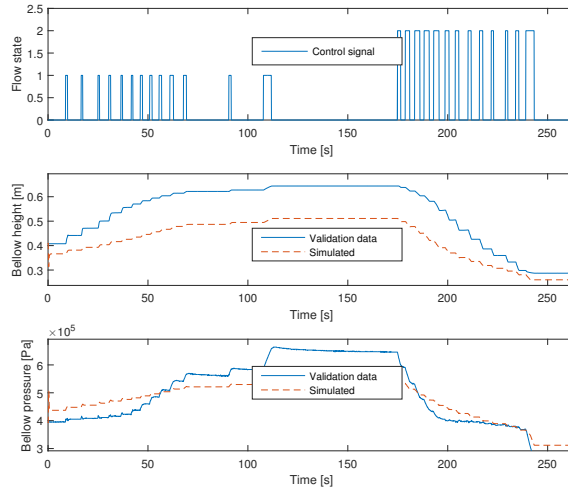

*Figure 5.38: Model 2 extended simulated and compared with data-set 2.*

Figure 5.39

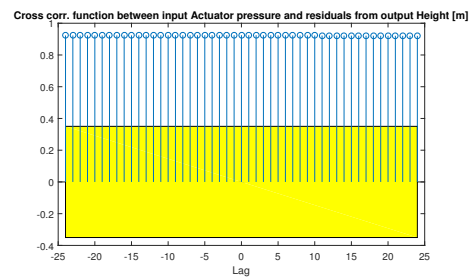**Validation of Model 2 extended with data-set 3**

Figure 5.40 shows the simulation results of the extended version of Model 2 with data-set 3. The same error as when simulated with the earlier models are presented. The residual analysis in Figure 5.41 - 5.44 indicates also here certain correlation between the input and the height residuals, especially concerning the actuator pressure input.
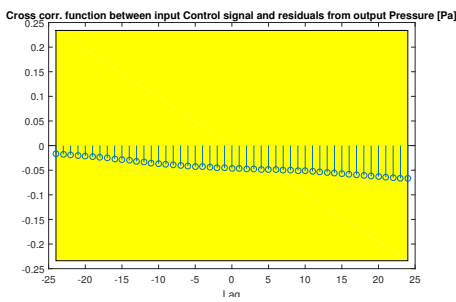

Figure 5.40: Model 2 extended simulated and compared with data-set 3.
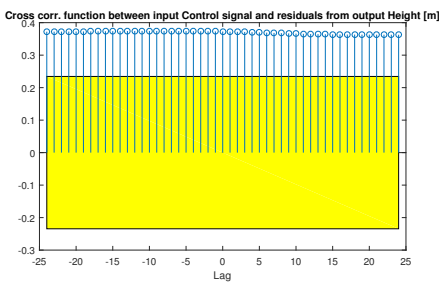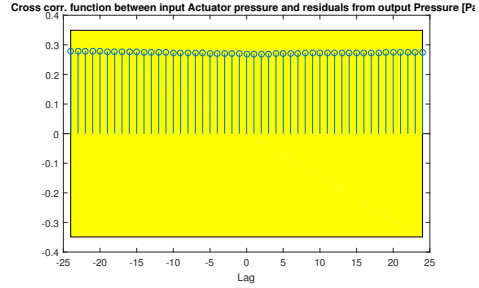

Figure 5.41: Cross correlation between control signal and height residual for extended Model 2 simulated with data-set 3, indicating a correlation between the height error and the control signal.

Figure 5.42: Cross correlation between pressure in actuator tank and height residual for extended Model 2 simulated with data-set 3, with values far outside confidence interval.
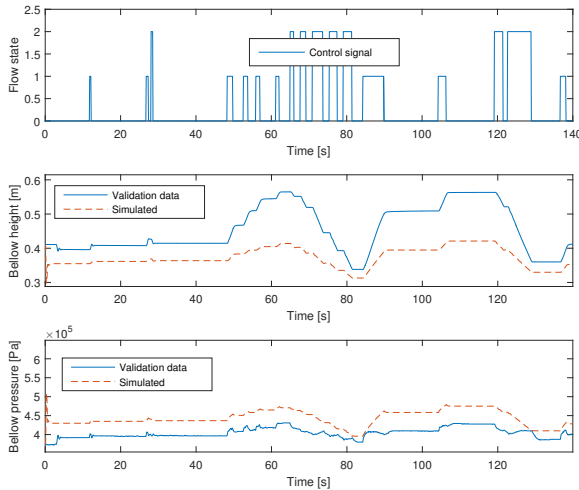
Figure 5.43: *Cross correlation between control signal and pressure, indicating low correlation.*
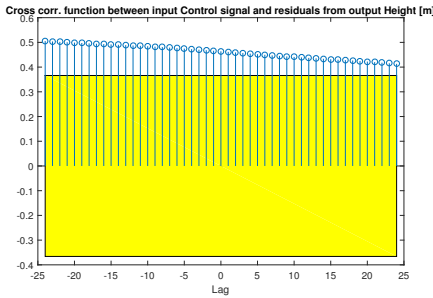

Figure 5.44: *Cross correlation between pressure in actuator tank and the pressure's residual, just inside of the confidence interval.*

Validation of Model 2 extended with data-set 4

In Figure 5.45 the results simulated with data-set 4 are presented, giving similar results as earlier presented simulations with other models. The resulting residual analysis is presented in Figure 5.46 - 5.49. Once again the residual analysis shows high indication of correlation between pressure in actuator tank and the output residuals.
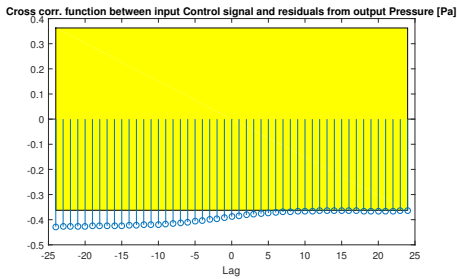

Figure 5.45: *Model 2 extended simulated and compared with data-set 4.*
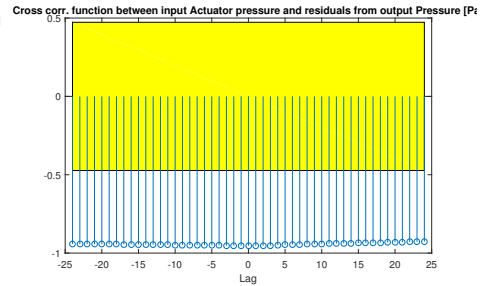
Figure 5.46: *Cross correlation between control signal and height residual for extended Model 2 simulated with data-set 4, indicating some cross correlation between the height error and the control signal.*
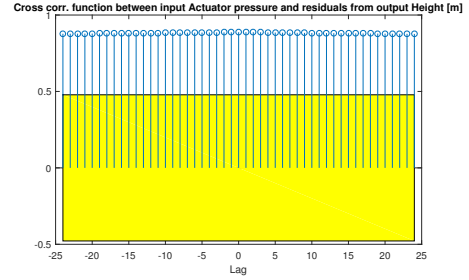
Figure 5.47: *Cross correlation between actuator tank pressure and height residual for extended Model 2 simulated with data-set 4, indicating a high correlation between the height error and the actuator pressure.*

Figure 5.48: *Cross correlation between control signal and pressure residual for extended Model 2 simulated with data-set 4, with values just outside of confidence intervall.*

Figure 5.49: *Cross correlation between actuator tank pressure and pressure residual for extended Model 2 simulated with data-set 4, indicating high correlation between the two.*

5.3.4   Model 3

The resulting NRMSE values from the validation of Model 3 is given in Table 5.16. It is clear that the model can not cope with the data-set 3-4, and therefore are the corresponding residual analysis not presented.

Validation of Model 3 with data-set 2-4

In Figure 5.50 - 5.52 Model 3's resulting simulation with data-set 2-4 are shown. The simulation with date-set 2 shows that the model can estimate the height quiet accurate, but fails with the data-set 3 and 4.

	data-set 2	data-set 3	data-set 4
NRMSE height	74.45 %	−46.35 %	−28.68 %
NRMSE pressure	74.00 %	61.51 %	−261.9 %

Table 5.16: *NRMSE values for Model 3 when simulated with validation data.*
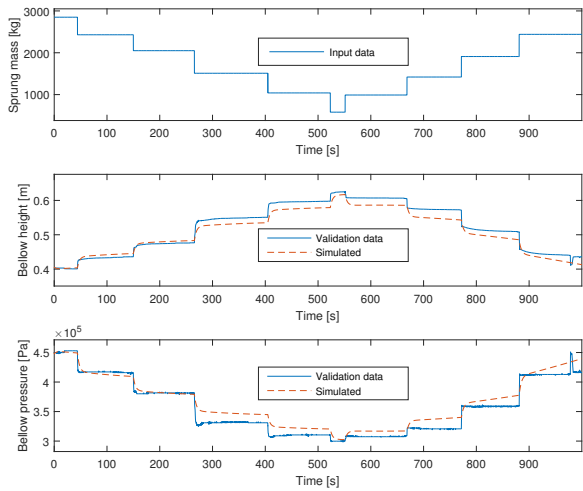
Figure 5.50: *Model 3 simulated and compared with data-set 2.*
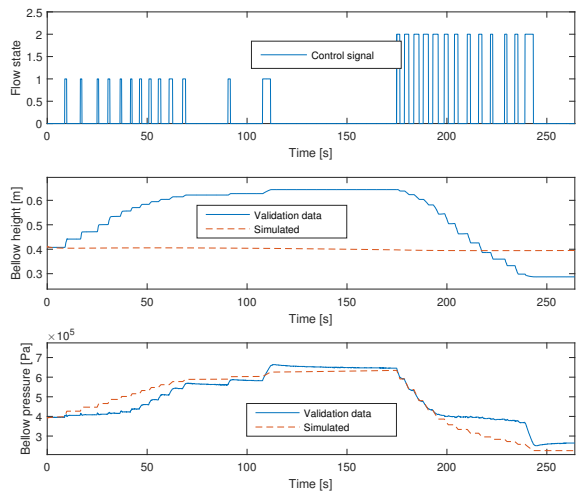
Figure 5.51: *Model 3 simulated and compared with data-set 3.*

Figure 5.52: *Model 3 simulated and compared with data-set 4.*

6

Discussion and Conclusion

In this section the models validity and possible error sources are discussed. Furthermore, what can be further evaluated is discussed. Finally, a conclusion is given, summarizing the success and the usability of the model.

6.1 Results

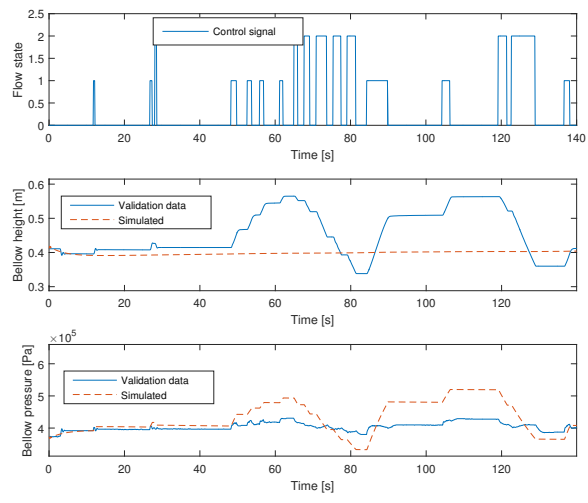The signal describing the steps in the load was created manually and the actual steps in mass are most probably slower than what the manually created signal suggests. It is therefore hard to conclude if any of the models succeed in simulating the fast dynamics well. However, both Model 1 and nonextended Model 2 gives a good static estimation of the height and pressure when load information is available and steps in the load are made, seen in Figure 5.26 and Figure 5.14. It is however clear that they do not capture the slow dynamics that can be seen in the same figures. The extended version of Model 2 captures the slow dynamics well and it provides a good static estimation of the height and pressure. The difference between the QCM 1 and QCM 2 methods seem to be negligible looking at the NRMSE values. Here greybox estimation of the effective area A_{eff} improves the low NRMSE values that Model 1 has initially. Both Model 1 and Model 2 show an undershoot in height and overshoot in pressure when loading mass. The reason might be that in reality the mass changes have a larger time constant. It might also be that friction is not modeled or not modeled well enough or limitations of the ideal gas law. Furthermore, it can be seen from the residual analysis from simulations with data-set 2 that some dynamics might be missing, especially between the mass input and the residual from the pressure output. This could be due to shortcomings in the cross sectional area estimation or that the temperature inside the bellow can not be assumed constant.

The slow dynamics of the system is most probably due internal friction when

the walls of the bellows are folding out or in. It is interesting that the slow increase in height does not result in a slow decrease in pressure. This is seen in earlier collected data, presented in Appendix A, that is not usable as it is not collected with the additional calibrated height sensor. This indicates that some experimental errors might be present. As the model of the slow dynamics depend on changes in the mass, this will be lost when simulated with data-set 3 and 4. The model would probably be better, and more general, if the input of the model would be dependent on changes in the height, corresponding better to a friction force.

When simulating Model 1, nonextended Model 2 and extended Model 2 with data-set 3 and 4 the models have an initial offset, as well as a continuing varying error. Data-set 1-4 have the same initial height and load, but both data-set 1 and 2 differ in initial pressure from data-set 3 and 4. This gives indications of hysteresis in the system or might be caused by an experimental error. This might be an error source for the poor results from simulations with data-set 3 - 4. Other error sources are probably also at fault for the poor results, one being the fact that the data used to estimate the air flow constants had to be approximated using both the ideal gas law and a numerical estimation of the derivative. Another could be shortcomings in the estimation of pressure in the actuator tank. The latter theory is supported by the fact that residuals indicate a high correlation between the bellow pressure and height residuals and the estimated actuator tank pressure.

Model 3 manages to estimate the height well in the first two steps in Figure 5.51 but struggles thereafter, probably due to nonlinearities that the system holds. It is clear that the model is not able to cope with data-set 3-4 and is not reacting to the change in pressure. Another problem with the estimated model is that there is no intuitive way to set the initial parameters, they have to be estimated using an iterative search for optimal solutions instead. This puts higher demands on computing resources, making it less attractive for online implementation.

It is clear from Figure 5.7 that the pressure not only depends on the height. An explanation could be that the average cross sectional area also depends on the load that is exerted on the bellow, making the walls of the bellow stretch out. It could also be caused by hysteresis, meaning that the pressure required for a reference height depends on if the bellow is expanding or contracting to this height. From the physical models it can be seen that a correlation between the pressure residual and mass input is present.

6.2   Future work

The possible future work of modeling the system can be divided into two approaches. One is to focus on physical models and further improve the sub-models presented in this thesis. with more and better measurements, for example measuring the air flow directly could be promising. The sub-models could be expanded and variables that have been assumed constant can be further investigated. The other approach is to further investigate statistical models, both non-

linear and linear models. Both approaches require collecting more data. For example, in order to model the system with only statistical methods, a lot of different explanatory variables (load, height, pressure in actuator tank) need to be considered when collecting data. New and more diverse validation data is needed to ensure an accurate model for both approaches, as well as a better estimation of the actuator pressure.

6.3   Conclusions

A general conclusion is that the system has nonlinearities, which also is supported by [14] and of course seen in the physical relations describing the system. The nonlinearities that are hard to include in the physical models is the fact that the air bellow moves in a circular manner and the air bellow is made out of an elastic material. Hysteresis in the function of the air bellow is reasonable but will complicate the model significantly.

Considering that the system depends on many surrounding variables, a statistical model demands a lot of data to cover every situation. Therefore it seems that the physical model is the better choice if a complete model of the system is sought after.

The goal of the thesis is to develop a model for the purpose of developing a controller algorithm and weight estimation. One of the physical models could be sufficient enough for the purpose of developing a controller algorithm or for the purpose of weight estimation. Although, for both estimation and model based controller purposes, a more accurate actuator pressure information is needed, either from estimation or from an additional pressure sensor.

A

The data in Figure A.1 is recorded while loading a truck equivalent to the truck used in data-set 1-4, measuring the height and pressure. In this data-set it is seen that the pressure presents a slow dynamic similar to the recorded height. This was not seen in the pressure in data-set 1-4. The data had to be discarded because of a faulty sensor.
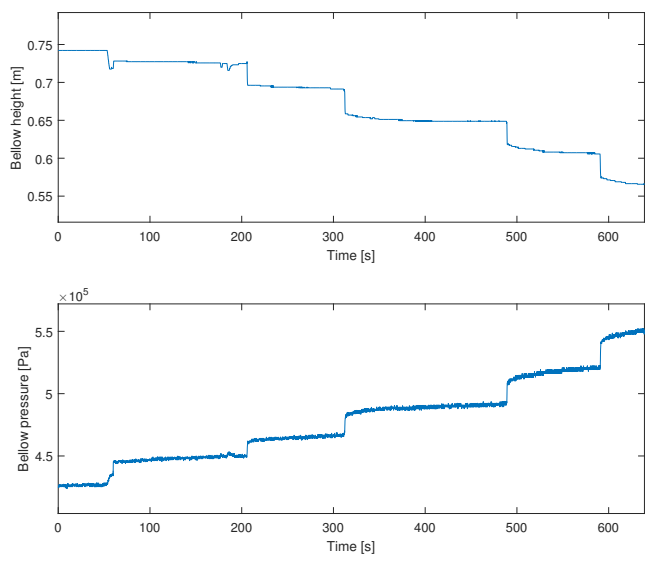
Figure A.1: *Discarded data measured with non-calibrated height sensor, suffering a off set.*

Bibliography

[1] Scania CV AB. Internal document, damper, . Cited on page 16.

[2] Scania CV AB, . URL `http://www.scania.se/om-scania/historia/`. Cited on page 1.

[3] Andrew Alleyne and J. Karl Hedrick. Nonlinear adaptive control of active suspensions. *IEEE TRANSACTIONS ON CONTROL SYSTEMS TECHNOLOGY*, 3(1), 1995. Cited on pages 12 and 16.

[4] A.J. Truscott & P.E. Wellstead A.W. Burton. Analysis, modelling and control of an advanced automotive self-levelling suspension system. *IEE Proc.-Control Theory Appl., Vol. 142, No. 2. March 1995*, 1995. Cited on page 16.

[5] M. Canale, M. Milanese, and C. Novara. Semi-active suspension control using ´´fast" model-predictive techniques. *IEEE Transactions on Control Systems Technology*, 14(6):1034–1046, 2006. doi: 10.1109/tcst.2006.880196. Cited on page 12.

[6] Hengjia Zhu Gang Tang and Yunqing Zhang & Ying Sun. Studies of air spring mathematical model and its performance in cab suspension system of commercial vehicle. *SAE International*, 2015. Cited on page 16.

[7] Lennar Ljung & Torkel Glad. *Modellbygge och simulering.* 2011. Cited on pages 3, 11, 18, 19, 20, 21, and 22.

[8] S. J. LEE. Development and analysis of an air spring model. *International Journal of Automotive Technology, Vol. 11, No. 4, pp. 471479*, 2010. Cited on page 16.

[9] Yang Nianjiong. Research on air suspension system based on pid control. *Fifth International Conference on Intelligent Human-Machine Systems and Cybernetics*, 2013. Cited on page 5.

[10] Yang Nianjiong. Research on air suspension system based on pid control. *2013 Fifth International Conference on Intelligent Human-Machine Systems and Cybernetics*, 2013. Cited on pages 12 and 16.

[11] Yunjun Li & Steve Opiteck Nikolai Moshchuk. Air suspension system model and optimization. *SAE International*, 2015. Cited on page 17.

[12] Stefan Sappei. Development engineer, scania cv ab, 2016. Cited on pages 6 and 7.

[13] Richard Vadasz. Development engineer, scania cv ab, 2016. Cited on page 7.

[14] Jie Xiao and Bohdan T. Kulakowski. Sliding mode control of active suspension for transit buses based on a novel air-spring model. *Proceedings of the American Control Conference*, 2003. Cited on pages 5, 18, and 57.

[15] Per Österman. URL `http://www.atl.nu/entreprenad/scania-kor-om-volvo/`. Cited on page 1.